Mechanisms of Bleomycin-Induced DNA Degradation†

JOANNE STUBBE*‡

Department of Biochemistry, College of Agricultural and Life Sciences, University of Wisconsin, Madison, Wisconsin 53706

JOHN W. KOZARICH§

Department of Chemistry and Biochemistry, University of Maryland, College Park, Maryland 20742

Received April 13, 1987 (Revised Manuscript Received June 25, 1987)

Contents

I. Introduction

During the past decade there has been an explosion in the research effort directed toward the isolation and evaluation of naturally occurring DNA cleaving agents and toward the design and synthesis of model compounds that can specifically recognize and cut DNA. The potential scope of the utility of these compounds is enormous and ranges from the creation of synthetic restriction enzymes for use by molecular biologists to the development of chemotherapeutic agents that may be effective against a variety of neoplastic diseases. Much of this interest has been fostered by an increasing awareness among chemists that DNA is a remarkably heterogeneous molecule. In addition to three distinct structural formats that double-stranded DNA can assume, there is striking internal variety within a single helix form. The rules that govern this heterogeneity are only beginning to be understood. Naturally occurring compounds such as metallobleomycin[1] (BLM) and neocarzinostatin[2] clearly have the ability to recognize and noncovalently bind to specific sequences in DNA and then to perform chemistry on a specific deoxynucleoside residue that can ultimately lead to strand scission. The studies of Sigman[3] using a 1,10-phenanthroline–copper complex [$(OP)_2Cu^I$], Dervan[4] with Fe·EDTA-containing systems, and Barton[5] with chiral transition-metal complexes demonstrated that the underlying principles governing the specificity and reactivity of a bleomycin-type compound can be applied

† Supported by Grant GM-34454 from NIH.
‡ J.S. is an NIH Research Career Development Awardee (Grant AM 01222) and an H. I. Romnes fellow from the University of Wisconsin.
§ J.W.K. is an American Cancer Society Faculty Research Awardee from the University of Maryland.

0009-2665/87/0787-1107$06.50/0

Professor JoAnne Stubbe received her B.A. in Chemistry from the University of Pennsylvania in 1968 and her Ph.D. at the University of California at Berkeley in 1971 (G. L. Kenyon, adviser). After a brief postdoctoral stint at UCLA with Jules Rebek, she joined the faculty of Williams College, Chemistry Department from 1972 to 1977, worked with R. H. Abeles at Brandeis University, and moved to Yale University as an Assistant Professor in Pharmacology, 1977–1980. She joined the faculty of the Department of Biochemistry at the University of Wisconsin-Madison in 1980, where she is now a full Professor. In September 1987, she will be a Professor in the Department of Chemistry, Massachusetts Institute of Technology.

John W. Kozarich (b. 1949) received a B.S. in chemistry from Boston College in 1971 and a Ph.D. in biological chemistry from MIT (NSF Predoctoral Fellow) in 1975. After a postdoctoral at Harvard University (NIH Fellow), he joined the Department of Pharmacology at Yale University School of Medicine in 1977, where he was promoted to Professor in 1984. Later that year he assumed his current position as Professor of Chemistry and Biochemistry at the University of Maryland, College Park. He is also an American Cancer Society Faculty Research Awardee. In addition to the mechanisms of DNA–drug interactions, his research interests include the mechanism and stereochemistry of enzyme reactions and the design of mechanism-based enzyme inhibitors.

to the design of relatively simple models.

This research also stimulated interest in the elucidation of the molecular mechanisms of drug-induced DNA degradation. Since the chemistry of DNA cleavage by these agents generally involves the fragmentation of the deoxyribose backbone by radical processes, the techniques employed to elaborate these mechanisms interface organic and inorganic chemistry, enzymology, and molecular biology. In this review, we will attempt to present an overview of the available information concerning metallobleomycin's structure(s), mode(s) of binding to DNA, and chemistry of cleavage of DNA. Although many key questions remain unanswered, our current understanding of the bleomycins provides a

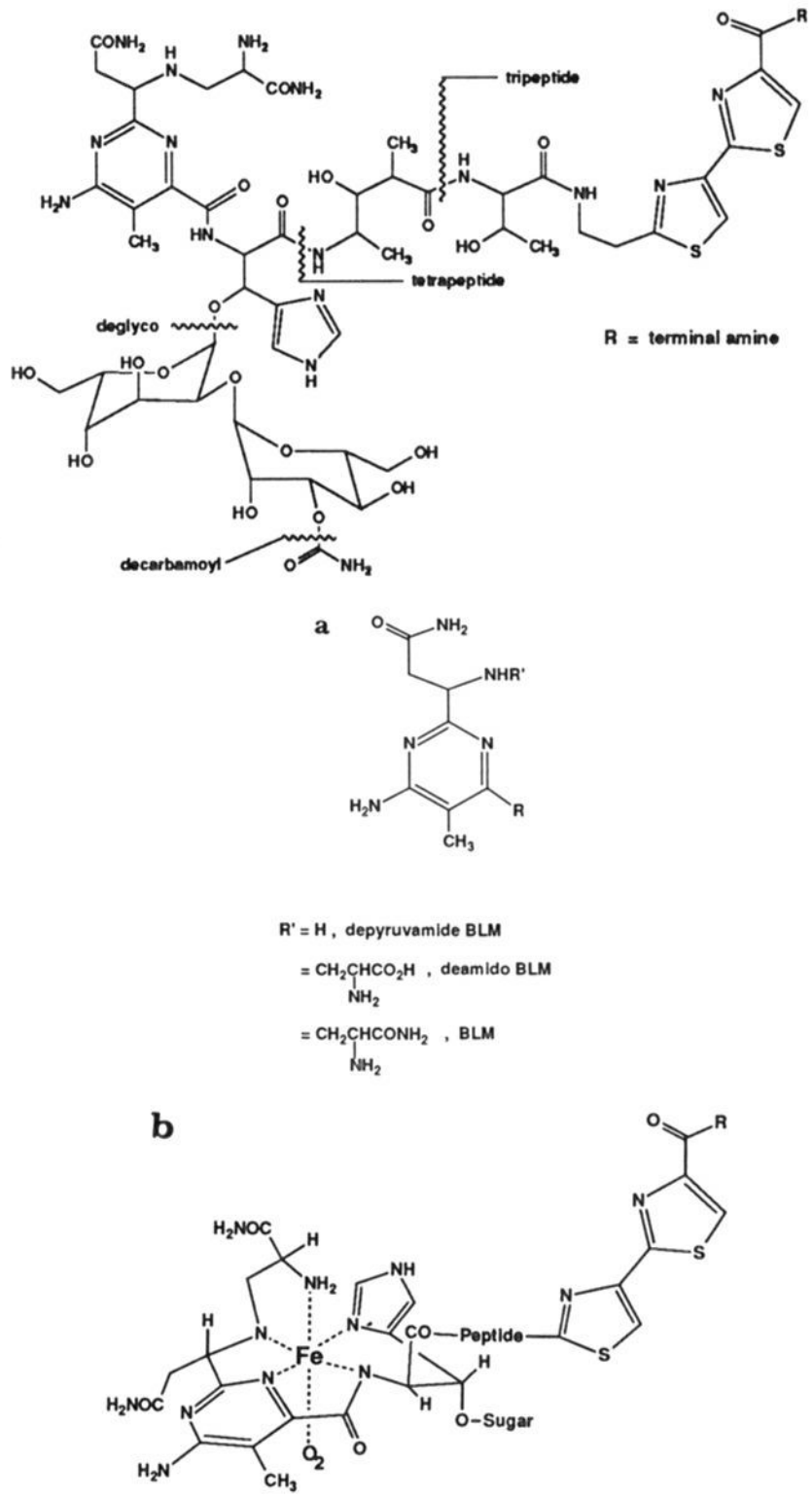

Figure 1. (a) Structure of bleomycin and its analogues. (b) Proposed structure for Fe(II)·BLM.

detailed framework that will be undoubtedly relevant to the study of other DNA-degrading agents. In this regard, the chemistry of related complexes, such as $(OP)_2$·Cu^I and methidium-propyl-EDTA·Fe(II) [MPE·Fe(II)] will also be discussed.

II. Bleomycin—The Prototypic DNA Cleaver: Structure and Domains

The bleomycins (Figure 1)[6–10] are a family of glycopeptide-derived antibiotics, discovered by Umezawa and co-workers, that have been used clinically against certain malignant lymphomas and squamous cell carcinomas. The therapeutic activity of the BLMs is generally believed to correlate with their ability to bind to and degrade DNA. Elegant studies by Sausville et al.[54] and a number of groups established that DNA strand scission requires O_2 and a metal ion, with Fe(II) being the most extensively studied and most active.[11–16]

Recent total synthesis of BLM by Takita et al.[17] and Aoyagi et al.,[18] as well as early chemical degradation studies by Umezawa et al.[9] to unravel the structure of BLM, allowed segregation of BLM into three domains. As indicated in Figure 1b, the pyrimidine, β-amino-

TABLE I. X-Band EPR and Visible Spectroscopy of Metallo-BLM Analogues[a]

compd	g_{11} (g_z)	g_1 (g_x, g_y)	A_{11}, G	λ_{max} (ϵ)	A^N_{11}, G
P-3A·Cu(II)[a]	2.214	2.133, 2.078	167.3	625 (125)[b]	
BLM·Cu(II)[a]	2.211	2.055	183	596 (120)	
deglyco-BLM·Cu(II)[a]	2.214	2.13, 2.077	167		
P-3A·Co(II)[a]	2.027	2.275	93.8		
BLM·Co(II)[a]	2.025	2.275	92.5		13
deglyco-BLM·Co(II)[a]	2.027	2.277	95.0		
iso-BLM·Co(II)[d]	2.025	2.270	93.0[d]		13
BLM·Co(II)·DNA[d]	2.026	2.272	92.5		13
P-3A·Co(II)·O_2[a]	2.107	2.007	22.4		
BLM·Co(II)·O_2[a]	2.098	2.007	20.2	450 (740)[c]	
deglyco-BLM·Co(II)·O_2[a]	2.100	2.009	22.5		
dep-BLM·Co(II)·O_2[d]	2.122	2.012	28.7		
BLM·Co(II)·O_2·DNA[d]	2.106	2.004	18.9		
P-3A·Fe(II)[a]				470 (320)	
BLM·Fe(II)[a]		no EPR		476 (380)	
deglyco-BLM·Fe(II)[a]				472 (300)	
BLM·Fe(III)·OH[e,f]	1.893	2.185, 2.431			
deglyco-BLM·Fe(III)·OH[e]	1.88	2.18, 2.432			
BLM·Fe(III)·OOH[e]	1.937	2.17, 2.254			
"Activated BLM"[g]	1.94	2.17, 2.26			
deglyco-BLM·Fe(III)·OOH	1.93	2.17, 2.25			
P-3A·Fe(II)·^{14}NO[a]	2.007	2.038, 1.968		470 (1800)	
BLM·Fe(II)·^{14}NO[a,g]	2.008	2.041, 1.976		470 (2300)	23.6
deglyco-BLM·Fe(II)·^{14}NO[a]	2.007	2.038, 1.964		475 (2200)	
iso-BLM·Fe(II)·^{14}NO[e]	2.008	2.040, 1.976			
deamido-BLM·Fe(II)·^{14}NO (pH 6.2)[e]	1.998	2.050, 2.013			17.6
deamido-BLM·Fe(II)·^{14}NO (pH 9.6)[e]	2.008	2.039, 1.969			23.8
dep-BLM·Fe(II)·^{14}NO[e]	1.999	2.052, 2.016			17.5
BLM·Fe(II)·^{14}NO·DNA[a]	1.962	2.060, 2.006			24.0

[a] Reference 24. [b] Reference 25. [c] Reference 26. [d] Reference 27. [e] Reference 28. [f] Reference 89. [g] Reference 68.

alanine, and β-hydroxyimidazole moieties are involved in formation of the metal complex that upon interaction with O_2 is responsible for DNA cleaving activity (domain 1). The actual structure of this complex continues to be the subject of extensive research and will be discussed in detail below. The bithiazole moiety, and perhaps the positively charged tail(s) of BLM, are required for DNA binding and sequence-specific recognition (domain 2, which will be discussed in detail in section IV).[19,20] The gulose and carbamoylated mannose residues (domain 3) are perhaps responsible for the selective accumulation of BLM in some cancer cells and are not required for the DNA cleaving ability of the drug.[21] The role of domains 1 and 2 of BLM will be discussed extensively in this review.

III. Metal Complexes of BLM

The coordination chemistry of Fe(II) and Fe(III)·BLMs has been intensely investigated since workers in the field realized that Fe(II) was essential for BLM-mediated DNA degradation in vitro. However, the nature of these ligands[22] and their arrangement in the Fe complexes still remain controversial. (The binding of the secondary amine, pyrimidine, and imidazole is not disputed. The ligation of the β-hydroxyhistidine amide and the carbamoyl group of mannose and their role in the coordination chemistry are controversial.) The coordination chemistry of other metallo-BLMs [Zn(II), Co(III)] have also been investigated by ^{13}C and ^{1}H NMR spectroscopy in an attempt to assign their structure and, by inference, that of the Fe(II) complexes. A recent excellent review by Dabrowiak[22] summarized the literature through 1981 and the conclusions to date concerning the coordination chemistry of metallo-BLMs. This section will focus on structural data not reported in this earlier review. No radical changes

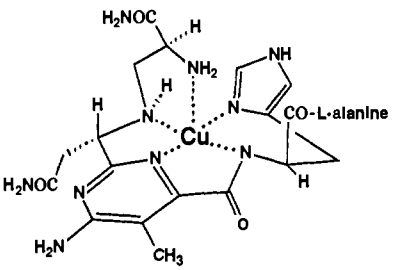

Figure 2. Proposed structure of Cu(II)·BLM.

in the proposed coordination chemistry have occurred since 1981.

The initial model for the expected coordination of metallo-BLMs was derived from the X-ray structure of a Cu(II) complex of a biosynthetic precursor of BLM, Cu(II)·P-3A (Figure 2).[23] This structure indicates that primary and secondary amines of the β-aminoalanine, the N1 of pyrimidine, and the N3 of imidazole are ligated to Cu(II) to produce the square-pyramidal (5:5:5:6 chelate ring) complex. Unfortunately, Cu(II)·P-3A lacks both the sugar residues (L-gulose and carbamoyl-D-mannose) and the bithiazole tail, raising questions as to its validity as a model for metallo-BLMs. Recent attempts have been made using X- and S-band EPR and ENDOR spectroscopy to establish the similarities or differences between Cu(II)·P-3A and Cu(II)·BLM.[24-28] The results from these studies, in which a variety of different metals were coordinated to P-3A, BLM, and deglyco-BLM, are summarized in Table I.

EPR spectra indicate geometric distortion of ligands around the metal, and the parameters reported for the P-3A and corresponding BLMs are remarkably similar. The g values for Cu(II)·P-3A and deglyco-BLM compared with BLM·Cu(II) appear slightly different, having rhombic g-anisotropies and decreased A_{11}'s. These differences have been interpreted to be due to lack of

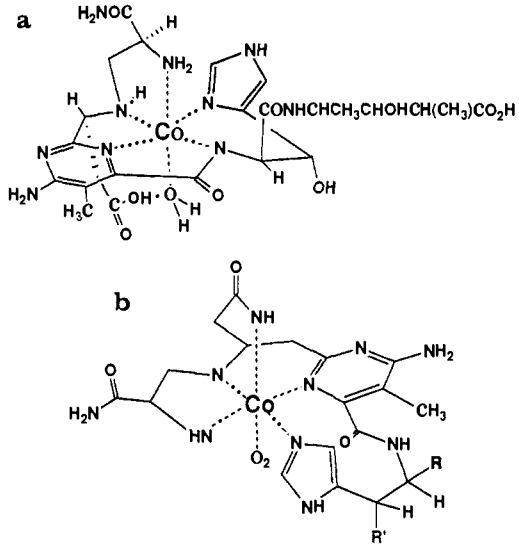

Figure 3. (a) Proposed structure of Co(III)·BLM.[30] (b) Alternative proposed structure of Co(III)·BLM.[31]

a sixth ligand.[25] Thus, these studies are consistent with strong similarities between Cu(II)·P-3A and Cu(II)·BLM. Studies using S-band EPR and ENDOR spectroscopic methods, which should improve the resolution of the hyperfine coupling with ligands and better define the ligands, are also consistent with the conclusion that coordination chemistry of Cu(II)·BLM is analogous to that observed in Cu(II)·P-3A.[29]

While the study of Cu(II) complexes provided a foundation for thinking about the coordination chemistry of other metallo-BLMs, the Cu(II)·BLMs are inactive in the degradation of DNA and therefore are perhaps of less interest than the Co(III)·BLMs and Fe(II)·BLMs. The Co(III)·BLMs were recently the focus of attention as potential diagnostic tools for tumor cell localization (^{57}Co·BLM), and most recently as a prototype for light-induced DNA degradation (see section VIIB). In addition, Co(III)·BLMs possess exchange-inert ligands and are diamagnetic and therefore have been the focus of ^{1}H and ^{13}C NMR spectroscopic investigations.

Co(III)·BLMs are typically prepared from Co(II)·BLM in the presence of O_2. This procedure results in the production of a number of Co(III)·BLM species (brown, green, orange) separable by HPLC. Dabrowiak and Tsukayama[30] recently isolated one major hydrolysis product (6 N HCl, 43 °C, 5 days) Co(III)·pseudotetrapeptide A-BLM (Figure 3a), starting with either the green or the orange Co(III)·BLMs. On the basis of ^{1}H NMR (DMSO and acidic D_2O) and CD and vis spectroscopic analysis, they concluded that Co(III)·pseudotetrapeptide A-BLM is isostructural with Cu(II)·P-3A (Figure 2). They also concluded from these studies that what distinguishes the green and orange Co(III)·BLMs is not part of the pseudotetrapeptide A of the antibiotic but additional ligation due to either the bithiazole tail or sugar moieties, and that the coordination chemistry observed for the hydrolysis product is a good structural model for the Fe·BLMs. This latter conclusion is based on several assumptions: (1) that the spectroscopic analysis of Sugiura et al. can be interpreted to indicate that Fe(II) and Co(II) are isostructural;[27] (2) that oxidation of Co(II) to Co(III) would "probably not alter ligand geometry"; (3) that Co(III) (d^6) is isostructural with divalent Fe(II) complex (d^6); (4) that under the hydrolysis conditions required to convert Co(III)·BLM(s) to Co(III)·pseudotetrapeptide A-BLMs, the ligands are indeed "exchange inert".

Conclusions concerning the structure of Co(III)·pseudotetrapeptide A-BLM from Dabrowiak's studies contrast with those drawn from earlier ^{13}C and ^{1}H NMR studies of Vos et al. on Co(III)·BLM.[31] They proposed a structure for Co(III)·BLM(s) that excludes the amide binding site and in which the pyrimidine and imidazole sites are cis in the metal polyhedron (Figure 3b). This cis coordination requires formation of a thermodynamically unfavorable nine-membered chelate ring. Further studies are obviously required to determine the structure of the photoactive Co(III)·BLMs and their relationship to Co(III)·pseudotetrapeptide A-BLM. Ultimately, X-ray structures of these species will be essential to resolve present discrepancies.

Besides the inherent interest in the structures of Co(III)·BLMs, they also might serve as reasonable models for the Fe·BLMs. On the basis of studies with Cu(II)·P-3A and Co(III)·pseudotetrapeptide A-BLM, an analogous arrangement of ligands was proposed for Fe(II)·BLMs (Figure 1b).

Insight into the geometry and coordination number of Fe·BLMs was obtained from extensive EPR studies of Sugiura[28] using a number of BLM analogues (Table I, Figure 1a). A case in point is the (1:1) nitrosyl adducts of Fe(II)·BLM and its analogues, which have properties quite similar to the extensively studied nitrosyl adducts of hemoproteins. The spectrum of Fe(II)·BLM is consistent with square-pyramidal geometry and one axial ligand. Addition of NO produces an EPR spectrum typical of 6-coordinate species, where NO has become the sixth ligand. NO has been used as a biophysical O_2 surrogate, and hence the Fe(II)·BLM·NO adduct is a good model for the first proposed intermediate in Fe(II)·BLM·O_2-mediated damage of DNA.

Comparison of the EPR parameters of nitrosyl adducts of BLM and iso-BLM and deglyco-BLM[28] indicates that they are almost identical and suggests that the carbamoyl group plays no coordination role in this complex. Comparison of the dep-BLM·NO parameters shows marked changes. Dep-BLM is missing the β-aminoalanine moiety of BLM and hence its proposed axial ligand (α-amino group of this moiety) in the Fe(II) complex. Interestingly, deamido-BLM exhibits EPR spectral properties that are pH dependent. At low pH (6.2) the nitrosyl complex is similar to the dep-BLM complex, while at high pH (9.6) it is similar to BLM. These results are also readily interpretable by changes in the axial ligand. Hydrolysis of the amide of the β-aminoalanine moiety of BLM changes the pK_a of the α-NH_2 moiety, proposed to be the axial ligand, from 7.7 to 9.3. Thus, at high pH the α-amino moiety can act as an axial ligand, consistent with its proposed role.

However, NMR studies by Oppenheimer et al.[32,33] on Zn(II)·BLMs and Fe(II)·BLM·CO resulted in the proposal of an alternative structure, analogous to the one proposed by Vos et al. (1980)[31] for Co(III)·BLM. In this proposed structure, the pyrimidine and imidazole ligands have a cis relationship, creating a nine-membered chelate ring. In further analogy, no role for the amide nitrogen of β-hydroxyimidazole is proposed. In addi-

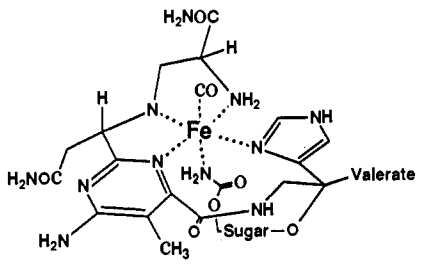

Figure 4. Proposed structure for Fe(II)·BLM·CO.

TABLE II. Cleavage Specificity of Dodecamer with BLM Analogues[36]

BLM	total events, $C_3 + C_{11}$, μm	specif, %	cleavage position, % C_3	C_{11}
Fe(II)·BLM A_2	62	78	15	85
Fe(II)·deglyco-BLM A_2	52	98	79	21
Fe(II)·decarbamoyl-BLM A_2	60	90	72	28

tion, a novel role for the carbamoyl group of the mannose portion of the sugar moiety as an axial ligand is suggested (Figure 4).

To obtain support for the carbamoyl group of mannose being involved in coordination, these authors also examined the NMR spectrum Fe(II)·CO·deglyco-BLM. As predicted, they observed differences in the β-aminoalanine moiety compared with either Fe(II)·BLM·CO or Zn(II)·BLM·CO complexes. In the case of deglyco-Fe(II)·BLM·CO, the CH–CH_2 relationship is gauche–trans, similar to that observed in the X-ray structure of Cu(II)·P-3A, also lacking the sugar moieties. This result contrasts with a gauche–gauche, CH–CH_2, relationship established for both the Zn(II)·BLM and Fe(II)·BLM·CO. The observed β-aminoalanine side chain conformational differences can be accommodated by the proposed differences in structures (compare Figure 4 with Figure 1b or 2). These NMR investigations thus raise two questions. How good a model is Fe(II)·CO·BLM compared with Fe(II)·NO·BLM for Fe(II)·O_2·BLM? Given the validity of the model, how important is the axial carbamoyl group to the chemistry, specificity, and product production?

Results, until recently, indicated that in spite of their coordination differences, both Fe(II)·BLM and Fe(II)·deglyco-BLM showed very similar specificities and extents of cutting for defined pieces of DNA.[24,33-35] [Differences are based on NMR data of Oppenheimer et al.[33] Similarities are suggested by EPR data (Table I).] However, a very recent report of Sugiyama et al.[36] studying the interaction of BLM-A_2, deglyco-BLM-A_2, and decarbamoyl-BLM-A_2 with a dodecamer provided some amusing results that address the role of the carbamoyl group in specificity. As indicated in Table II,

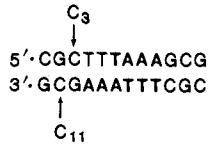

the specificity of cleavage (proportion of oligonucleotide modification occurring at C_3 plus C_{11}) and the chemical products[37] are the same for all three BLMs. However, the ratio of C_3/C_{11} cleavage varied dramatically. For BLM, maximum cleavage occurred at C_{11}; while for both deglyco-BLM-A_2 and decarbamoyl-BLM, lacking the carbamoyl ligand, maximum cutting was observed at C_3. The simplest interpretation advanced for the observed cleavage patterns is that BLMs can bind to GC pairs in DNA in two complementary orientations. The carbamoyl group appears to play an important role in orientation, by a mechanism which may or may not involve coordination to the Fe(II).

In summary, the general consensus resulting from intensive investigations on metallo-BLMs is that N1 of the pyrimidine, N of imidazole, and the secondary amine are ligated to the metal. The arrangement of these ligands and the nature of the remaining ligands are still controversial, especially the roles of the α-amino group of the β-aminoalanine moiety and the amide nitrogen of the β-hydroxyimidazole. In the case of the Fe(II)·BLM, it may be possible that ligand reorganization accompanies Fe(II) activation.

IV. Binding of BLM to DNA

Recent total convergent synthesis of BLM by Takita et al.[17,38] and Aoyagi et al.[18,39] showed that BLM is composed of three domains. One domain, the bithiazole moiety, and perhaps the charged residue adjacent to this moiety, was shown to be responsible for binding of BLM to DNA. The K_as for BLM and the corresponding tripeptide-S (Figure 1), in the absence of metal ions, under similar conditions, was reported to be 1.2×10^5 M^{-1} [40] and 1.4×10^5 M^{-1},[41] respectively. While there is little dispute about the major role of the tripeptide-S in binding to DNA, the mode(s) of binding are more controversial. A number of laboratories utilized a variety of complementary techniques to investigate the possibility that the bithiazoles are responsible for intercalative binding.[42] These techniques include (1) gel electrophoresis and sedimentation methods to measure the unwinding (relaxation) of supercoiled DNA and then overwinding;[20,41] (2) linear dichroism methods and viscometric methods to measure the lengthening of linear DNA;[40,41] (3) NMR spectroscopy to measure the shifts of resonances associated with the drug on binding to DNA.[40,43,44] All of these methods lead to the conclusion that more than one mode of binding of BLM to DNA occurs.

1. Relaxation of supercoiled DNA and reversal of supercoiling in the presence of BLM (pH 5.5) and tripeptide-S (pHs 5.5 and 8.0) were measured by Povirk (1979)[41] using sedimentation methods. The low pH was utilized in an attempt to avoid BLM-mediated nicking of supercoiled DNA. Similar studies using tripeptide-S, where degradation was not a complicating problem, gave the expected relaxation followed by positive supercoiling of DNA. Povirk also determined the DNA unwinding angle, caused by tripeptide-S binding, to be 12°/molecule. This value is smaller than most intercalators, for example for ethidium, $\phi = 26°$.[42]

A number of bithiazole derivatives indicated in Table III were also used as models for investigating BLM binding modes.[19,20] Work of both Fisher et al.[20] and Kross et al.[19] showed that many of these derivatives uniformly inhibit breakage of DNA by BLM without affecting its specificity. These results contrast with other unrelated intercalators (ethidium, distamycin)[45] and antitumor agents such as *cis*-platinum,[46] all of, which modify BLM's specificity. DNA binding of these bithiazole derivatives (Table III) was studied by two

TABLE III. Cationic Bithiazoles Interaction with DNA

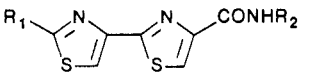

R^1	R_2	M^c	unwinding/rewinding
$CH_3CONHCH_2CH_2$	$(CH_2)_3S^+(CH_3)_2$	5×10^{-3} [a,b]	+
$CH_3CONHCH_2CH_2$	$(CH_2)_4N^+H_3Cl^-$	10^{-4}–5×10^{-3} [a]	+
C_6H_5	$(CH_2)_3S^+(CH_3)_2$	10^{-4} [a]	+
4-thiazolyl	$(CH_2)_3S^+(CH_3)_2$	10^{-4} [a]	+
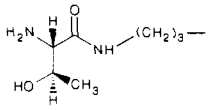	$(CH_2)_3S^+(CH_3)_2$	[b]	
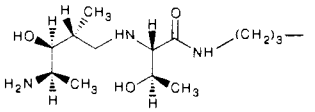	$(CH_2)_3S^+(CH_3)_2$	3×10^{-5} [b]	
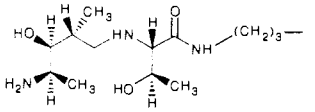	$NH(CH_2)_4NHC(NH)(NH_2)$	2×10^{-4} [b]	
$NH_2(CH_2)_2$	$NH(CH_2)_3(NH(CH_2)_4NH_2$	6×10^{-6} [b]	

[a] Reference 91. [b] Reference 114. [c] 50% inhibition of Fe·BLM-mediated DNA degradation.

complementary topological methods.[20] The bithiazole derivatives examined promote helix unwinding and overwinding (positive supercoiling) and provide evidence in support of a partial intercalative binding mode.

2. Helix extension in the presence of drug is also a standard criterion for intercalation. However, the observed extension can fall anywhere between 1.8 to 4.5 Å for known intercalators.[42] The characteristic time (μs) for rodlike DNA to orient in an electric field, monitored by linear dichroism, was used by Povirk et al.[41] to determine the length of DNA in the presence of BLM and tripeptide-S. Each tripeptide-S bound lengthened DNA by 3.1 Å, well within the observed range of other intercalators.

Lengthening of DNA by bound BLM was also measured by viscometric methods.[40] In contrast to the expected increase in viscosity for a compound that binds by intercalation, no change in viscosity was observed.

3. A partial intercalative mode of binding is also supported by studying the interaction of BLM-A_2 and a variety of bithiazole derivatives with poly(dAdT) by NMR spectroscopy. The bithiazole proton resonances and the methyl hydrogens of the sulfonium group are broadened and shifted to a higher field. The magntiudes of these high-field shifts vary with different bithiazole derivatives and perhaps the degree of intercalation.[40,43] In addition, the small magnitude of the chemical shift perturbations argues against classical intercalation. The influence of temperature, pH, and ionic strength on the binding of bithiazoles to DNA, assessed by NMR methods, suggested that more than one mode of binding exists.[43] Lack of perturbation of the dT(H-6) or dT(CH_3-5) on BLM binding to poly(dAdT) suggests minor groove interaction.

Additional support for two modes of binding by BLM comes from studies of Huang et al. (1980),[47] who showed that there exist two types of DNA-induced fluorescence quenching of BLM-A_2. One type is sensitive to and the other type is insensitive to changes in ionic strength. The nonionic type may be associated with partial intercalation of the bithiazole rings and the ionic type with binding of (+)-charged tail with the negative phosphate backbone. No correlation, however, could be established between either mode of quenching and ability to degrade DNA. Interestingly, phleomycin, which contains a reduced and hence a nonplanar bithiazole ring, also degrades DNA with specificity similar to BLM.[48] These results also suggest alternative modes of binding to intercalation.

Whether BLM binds via intercalation and the iron chelating end of the molecule is accessible to the minor groove, or whether BLM binds in the minor groove, cannot be present be differentiated. However, the observation that BLM mediates exquisitely specific 4′-carbon–hydrogen bond cleavage to oxidatively degrade the deoxyribose moieties of B-form DNA is consistent with and provides the strongest support for BLM-mediated attack within the minor groove of DNA.

As outlined above, extensive investigations attempted to define the mode(s) of BLM binding to DNA. The ultimate goal of these studies is to explain the observed preference for single-strand scission at GpC, GpT sequences on linear DNAs[12,13] and the observed preference for double-strand scission at sequences[49]

Pyr·G-C·Pur
Pur-C·G·Pyr·

A recent review by Dickerson[50] reported preliminary computer modeling of BLM binding to the dodecamer d(CGCGAATTCGCG) in an attempt to account for both binding and specificity information discussed above. The model shown has the bithiazole rings binding in the minor groove (Figure 5). This proposal is based on their observations that the bithiazole tail of BLM is very similar to the fluorescent dye Hoechst 33258 in size, shape, positively charged end, and hydrogen-bonding propensity. Recently this group showed by X-ray analysis that Hoechst 33258, which binds tightly to DNA, binds in the minor groove of the dodecamer in a manner analogous to netropsin (Figure 6).

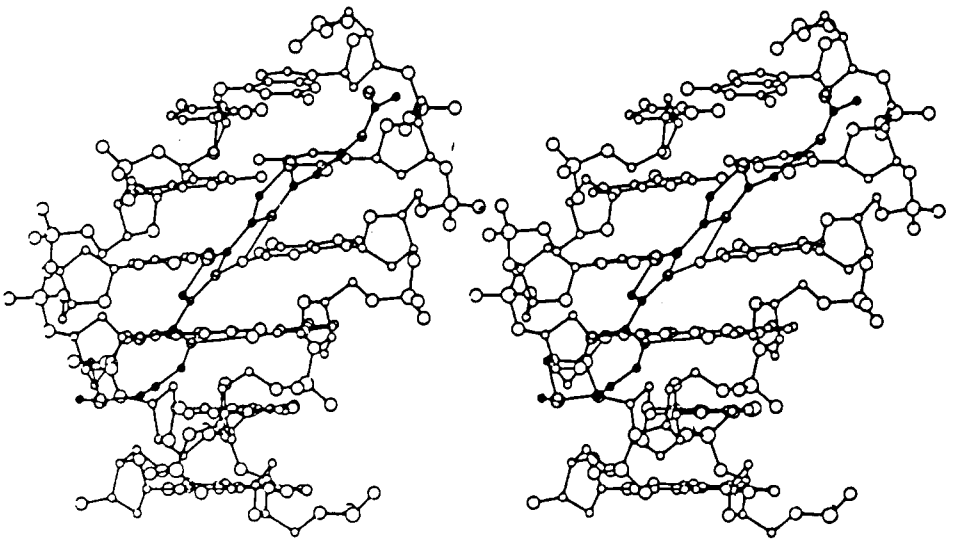

Figure 5. Stereopair computer drawing of the hypothetical complex of the bithiazole group from bleomycin with an alternating GC double helix of B-DNA. Thin lines represent hydrogen bonds.

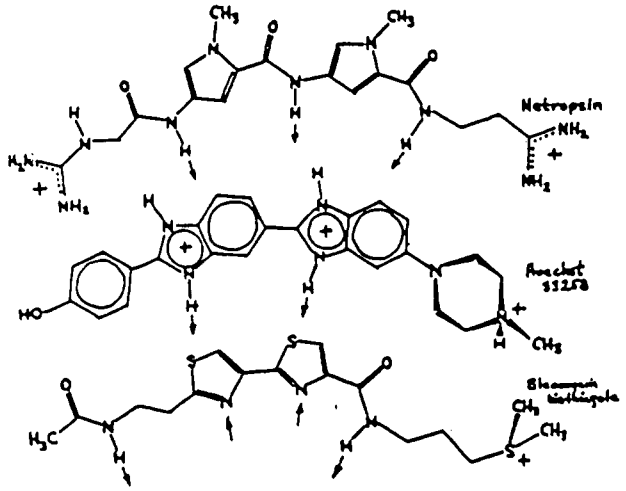

Figure 6. Comparison of skeletons of netropsin, Hoechst 33258, and the DNA-binding bithiazole portion of bleomycin A_2. Arrows indicate potential hydrogen-bond donors or acceptors. Note the common crescent shape of the three molecules.

While much new insight about DNA–BLM interactions has been obtained, it is clear that further experiments such as those recently reported by Kowabara et al.[51] with $(OP)_2Cu^I$ and Dasgupta and Goldberg[52] with neocarzinostatin need to be undertaken to establish the mode of binding of BLM to DNA to account for both binding and chemical specificity.

V. Chemistry of Fe(II)·BLM

The elegant studies of Sausville et al.[53,54] elucidated the essential requirements for the cofactors Fe(II) and O_2 in BLM-mediated degradation of DNA in vitro. These studies also showed that formation of a 1:1 Fe(II)·BLM complex was required for the production of free base and malondialdehyde-like material in the presence of DNA. Haidle et al.[57] and Kuo and Haidle[58] had previously demonstrated production of free nucleic acid bases and aldehydic materials resulting from incubation of BLM with DNA. However, the work of Sausville et al.[53,54] demonstrated that Haidle's observed products, which required the presence of organic reducing agents, were related to "adventitious Fe(II)"

SCHEME 1

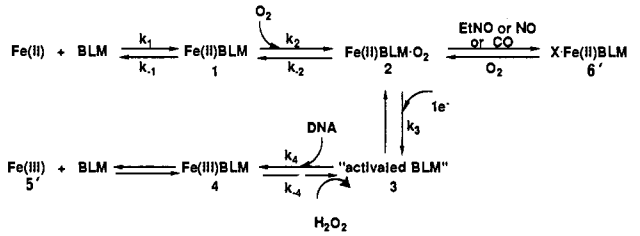

present in their reaction mixtures. The reductants, therefore, were required to convert Fe(III) to Fe(II), the cofactor for the BLM reaction in vitro.

The established requirements for Fe(II) and O_2 triggered a large number of investigations in an attempts to unravel the chemistry of the Fe(II)·O_2·BLM species responsible for production of the products observed upon interaction of the complex with DNA or with small molecules (olefins, dimethylaniline, cumene, etc.). This section outlines the evidence in support of a high-valent iron–oxo species being responsible for both the characterized spectroscopic intermediates and the observed chemical reactivity. BLM offers a unique opportunity to study a nonheme iron system, capable of mediating chemistry perhaps analogous to the intensively investigated heme-containing oxygenases, including cytochrome P_{450} (cyt P_{450}), horseradish peroxidase, chloroperoxidase, and heme model chemistry.[59-63]

A. Kinetics and Characterization of Intermediates Kinetically Competent To Degrade DNA: Biophysical and Spectroscopic Methods

The use of a combination of biophysical techniques, including stopped flow spectroscopy, EPR and Mossbauer spectroscopy, allowed Burger et al.,[64,65] Sugiura and Kikuchi,[66] and Kuramochi et al.[67] to propose a scheme to account for BLM-mediated degradation of DNA. The proposed sequence of events responsible for production of "activated BLM", the species responsible for oxidatively degrading DNA, is outlined in Scheme 1 (see also Table IV). Fe(II) combines with BLM to produce an EPR silent, high-spin Fe(II)·BLM complex (Table V).[14,67,68] This species then rapidly and rever-

TABLE IV. Kinetics for Formation and Degradation of Activated BLM

	temp, °C	rate constant
k_2	2	3.47 s^{-1} [a]
k_3	2	0.12 s^{-1}
k_4	6	0.006 s^{-1} [b]
	0	0.002 s^{-1} [d]
k_3	6	0.5 M^{-1} s^{-1} [c]

[a] Assuming O_2 is saturating. Reaction is first order in O_2 and Fe(II)·BLM (ref 68). [b] The same k_4 is observed in the presence or absence of DNA. [c] Reference 64. Reaction is much slower than Fe^{II}·O_2 reaction and kinetic data not very reliable. [d] Reference 67.

TABLE V. Spectral Characteristics of Species Observed in Fe(II)•BLM

complex	UV·vis	EPR	Mössbauer
1	370, 476 (pink) (ϵ = 380 M^{-1} cm^{-1})	silent	high-spin (s = 2)
2	385	silent	quadruple splitting, $\Delta E\phi$ = 2.96 mm/s; isomer shift δ = 0.16 mm/s
3	365, 384	g = 2.26, 2.17, 1.94,[a,c] 2.0046[c]	low-spin Fe(III)
4	365, 384	g = 2.45, 2.18, 1.89	
5		g = 4.3	
6	[EtNC] 497[b] (ϵ = 3.0 mM^{-1} cm^{-1}); [CO] 384[b] (ϵ = 2.7 mM^{-1} cm^{-1}); [NO] 470 nm[b] (ϵ = 2.3 M^{-1} cm^{-1})		

[a] Reference 68. [b] Reference 14. [c] References 66, 182.

sibly forms a ternary Fe(II)·O_2·BLM complex, whose Mossbauer parameters have been described and are most consistent with a ferric superoxide structure.[65] The reversibility of the formation of this ternary complex is convincingly demonstrated with carbon monoxide, ethylisocyanide, and NO, which inhibit activated BLM production by forming Fe(II)·X·BLM, but upon removal and addition of O_2 allow its formation.[14] The production of activated BLM from complex **3** requires a one e^- reduction. This e^- can be supplied by Fe(II)·BLM or by organic reductants. In addition, activated BLM can also be produced from HOOH or EtOOH and Fe(III)·BLM.[14] The activated BLM produced via H_2O_2 appears to be identical with that produced by the Fe(II), O_2, reductant pathway, based on EPR and Mossbauer characterization,[14,65] as well as the similarity in products produced by both pathways.[69] The structure of activated BLM was characterized further by using ^{57}Fe (I = 1/2), $^{17}O_2$, and EPR spectroscopic methods. A ^{57}Fe nuclear hyperfine splitting of 22 G in the g = 1.94 spectral feature of activated BLM is observed. Such a large splitting would be observed only if the unpaired spin is localized on iron.[14] Similarly, if activated BLM is produced from Fe^{II}.$^{17}O_2$ (^{17}O, I = 5/2), the presence of oxygen in this complex is defined by the observed broadening of the g = 2.17 feature and indicates that rapid exchange of ^{17}O label with solvent is not encountered. Unfortunately, these studies do not allow a distinction to be made between the presence of one or two oxygens in the activated complex. Such a distinction might be made by looking for the O–O stretch vibration of metal-bound species using either infrared or resonance Raman spectroscopy and confirmation using isotopic substitution.[70] Given

CHART I

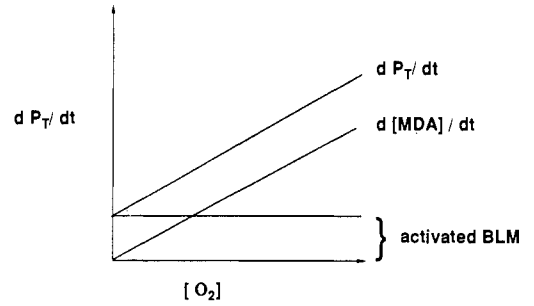

the lifetime of the observed activated BLMs, this approach to elucidating the structure of the "active" species should be investigated. The EPR and Mossbauer data also indicate that the Fe(III) in the activated complex is low spin. This spectroscopic data allowed Burger et al. (1981)[14] to propose that activated BLM might have a structure analogous to compound I of peroxidases or the single e^- reduced species of oxy-cyt P_{450}. Very recent studies using 1-e^- (potassium iodide) and 2-e^- (thioamide analogue of NADH) reductants[71] indicated that activated BLM contains two additional oxidizing equivalents compared with Fe(III)·BLM. These results are consistent with the proposal of Burger et al.[14] that activated BLM is a high-valent "Fe^V=O" species. [In this review Fe^{III}Ö:: and [Fe·O]$^{3+}$ are equivalent to Fe^V=Ö:, and these have been used interchangeably. While Mossbauer studies suggest that $Fe^{III}O$[65] is the best formulation of activated BLM, the actual structure of the species involved directly in C–H bond cleavage is unknown.] We will return, subsequently, to the structure of activated BLM and provide additional support for high-valent iron species (Fe^V=O) when considering its chemical reactivity with small molecules and DNA in comparison with well-characterized heme oxygenases.

The slow step in Fe(II)·BLM-mediated DNA degradation (Scheme I) is proposed to be decomposition of activated BLM as measured by production of both types of monomeric products. The validity of this proposal is testable by using a classic partitioning experiment (eq 1) similar to those described to study the mechanism of ester and amide hydrolysis by chymotrypsin.[72] This model would predict that as the con-

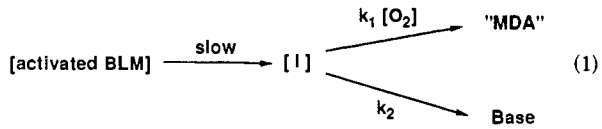

(1)

centration of oxygen in solution is increased that the rate of both base propenal and total product production (base and base propenal) should increase (Chart I). Experiments are in progress to test this model.

After chemical reaction with DNA, low-spin (S = $^1/_2$) (Table V) Fe(III)·BLM is observed by EPR spectroscopic methods, which in the absence of reductant reverts to rhombic Fe(III), g = 4.3 (S = $^5/_2$). The possibility that activated BLM is [Fe^{III}Ö::] is also supported by studies of Burger et al.[14] and Kuramochi et al.,[67] which indicated that activated BLM, incubated in the absence of DNA for several minutes, loses its ability to degrade DNA. Attempts to reactivate BLM also failed, and therefore BLM appears to mediate its own self-destruction.

TABLE VI. Summary of the Chemical Reactivities of Ferric Bleomycin as Compared with Chloroperoxidase and Cytochrome P_{450}

	phenylperacetic acid decarboxyln	cumene hydroxyln	olefin epoxidn	*m*-CPBA-supported oxygen evoln	peroxide-supported MCD chlorin	peroxide/peroxyacid-supported *N*-demethyln of DMA	*N*-oxide-supported *N*-demethyln of DMA	peroxidn of *O*-dianisidine
bleomycin	–[a]	–[a]	+[b]	+[a]	+[a]	+[a]	–[a]	+[a]
cytochrome P_{450}	+[c]	+[c]	+[c]	–[a]	–[a]	+[d]	+[e]	+[a]
chloroperoxidase	–[c]	–[c]	+[c]	+[e]	+[f]	+[g]	–[g]	+[a]

[a] Reference 76. [b] Reference 84, 85. [c] Reference 186. [d] Reference 187. [e] Reference 188. [f] Reference 189. [g] Reference 190.

SCHEME 2

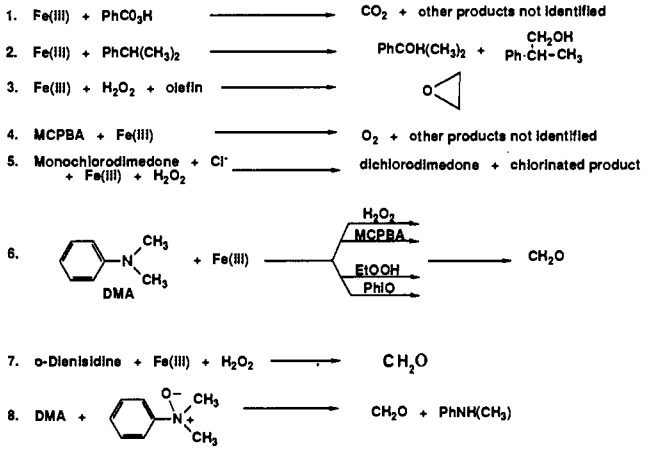

These results are remarkably similar to those reported by Guengerich[73] that cyt P_{450}'s rapidly inactivate themselves in the absence of substrate, producing modified protein residues and modified protoporphyrin IX. Preliminary studies of Takita et al.[74] indicated that inactivation of BLM is accompanied by modification of the pyrimidine moiety. ^{13}C NMR studies of Dabrowiak et al. also supported this thesis.[75] Elucidation of the structure(s) of the modified species might better define the structure of activated BLM.

B. Chemical Methods To Characterize Activated BLM

Since activated BLM was proposed to be similar to compound I of the peroxidases and/or "active" cyt P_{450}, Padbury and Sligar[76] investigated the possibility that Fe(III)·BLM oxidant could catalyze six oxidative reactions characteristic of heme proteins.

The reactions investigated are shown in Scheme 2, and their results are summarized in Table VI.

A cursory glance at the results in Table VI indicates that Fe(III)·BLM appears to have chemical properties more closely related to chloroperoxidase than to cyt P_{450}. However, care must be taken with this interpretation, as in many cases the relative rates of product production in the various systems differ by several orders of magnitude (10^3–10^4), and the conditions of the individual reactions have not been optimized. Both peroxidases and cyt P_{450} in fact may catalyze the production of the same "active FeO" species; however, the chemistry observed is probably related to the marked difference in amino acid residues in their active site binding pockets.[77,78] In addition, the observation that Fe(III)·BLM in the presence of either H_2O_2 or a peracid cannot effect hydroxylation of cumene is perhaps an unexpected and interesting result, given that a substantial body of evidence now supports a similar hydroxylation of the C4′ position of the deoxyribose moiety of a pyrimidine in DNA as a requirement for free base release.[69] Thus, while comparisons between the heme system and BLM systems are tempting, caution is warranted to avoid overinterpretation.

In the past 6 years interest in understanding the biological strategies for oxygen metabolism has resulted in synthetic metalloporphyrin models of these processes.[59] Synthetic porphyrins have now been developed that can catalyze many of the reactions in the repetoire of cyt P_{450} (hydroxylations, olefin epoxidation, hetero atom oxidation, etc.). Studies on these model systems have provided new insight into detailed mechanisms of these reactions as well as the foundation for thinking about similar chemistry in enzymatic systems.[61–63,79,80]

While the emphasis in the recent past has been on "heme" systems, it is rapidly becoming clear that in nature each heme system has a nonheme counterpart.[81] The vast methodology utilized to study metalloporphyrins can now be applied to nonheme equivalents such as metallo-BLMs, and this approach was recently taken by Hecht and co-workers.[82–85] They cataloged the types of reactions that can be mediated by activated BLM generated by using Fe(III)·BLM and a variety of oxidants, including iodosobenzene, sodium metaperiodate, H_2O_2, cumene hydroperoxide, and/or Fe(II), O_2, and ascorbate (Chart II). The former oxidants used in ferric activation were previously investigated as oxygen surrogates in the cyt P_{450} reactions as well as in porphyrin in model systems.[61–63] Several important results from these papers require consideration.

First, much debate concerning the cyt P_{450} studies utilizing a variety of oxidants focused on whether the active Fe·O species is identical in all cases regardless of oxidant (iodosobenzene, alkyl peroxides, peracid, etc.). In fact, elegant model studies of Lee and Bruice[86] showed that interactions of porphyrins with peracids and alkyl peroxides proceed via different mechanisms, the peroxides involving deprotonation[87] and homolysis and the peracids involving protonation of the leaving group and heterolysis, to produce the activated species. While the nature of the active metal–oxo species is unknown in "active BLM", the similarity of product distributions observed for a variety of oxidants is suggestive of a common intermediate. Similarly, Padbury and Sligar[88] (personal communication) measured identical isotope effects on oxidation of dimethylaniline to formaldehyde by a variety of oxidants (Table VII). These results again suggest a common intermediate produced by all oxidants.

Second, monoxygenases were shown to mediate hydroxylations of a variety of aromatic substrates.

CHART II. Reactions Catalyzed by Activated BLM[a]

	oxidant	substrate	products (percent yields)			
1 a)	Fe(III)BLM PhIO	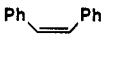	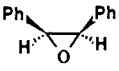 1 (20)	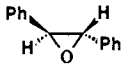 2 (8)	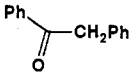 3 (5)	PhCHO 4 (5)
b)	$NaIO_4$		1 (12-18)	2 (0)	3 (10-15)	4 (5)
c)	EtOOH	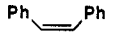	1 (17)	2 (2)	3 (7)	
2	Fe(III)BLM PhIO	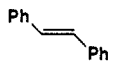	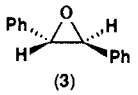 (3)	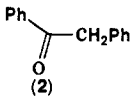 (2)		
3	Fe(II)BLM, O_2 ascorbate	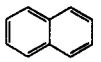	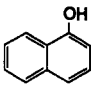			
4	Fe(II)BLM, O_2 ascorbate	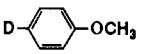	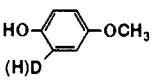			
5	Fe(III)BLM PhIO	DMA	$PhNHCH_3$ + HCHO			
6	Fe(II)BLM, O_2 ascorbate	DMA	$PhNHCH_3$ + HCHO			

[a] References 82–85.

TABLE VII. Isotope Effects on the Oxidation of Dimethylaniline to Formaldehyde by "Activated BLM" Generated by Various Oxidants

oxidant	isotope effects d^{3a}	isotope effects d^{6a}
Fe(II), O_2, ascorbate	<3.5	
Fe^{III}-H_2O_2	3.12	3.3
Fe^{III}-EtOOH	2.13	3.17
Fe^{III}-*t*-BuOOH	2.12	3.06

[a] d^3, d^6 refer to *N*-(methyl-d_3)-*N*-methylaniline and *N*,*N*-di(methyl-d_3)aniline.

Mechanistic studies implicated arene oxide intermediates in these reactions, because of the observation of a 1,2 H shift from the site of oxidation that accompanies hydroxylation. A second, interesting observation of Murugeson and Hecht[83] is that active BLMs have the ability to mediate an NIH shift. They showed that incubation of (80%) *p*-deuterioanisole with Fe(II)·BLM·O_2 and ascorbate produced *p*-methoxyphenol containing deuterium (15–20%).

Finally, product analysis of the reaction of *cis*-stilbene with Fe(III)·BLM and an oxidant (H_2O_2, iodosobenzene, $NaIO_4$) indicates formation of benzaldehyde and *trans*-stilbene[82] in addition to *cis*-stilbene oxide and $PhCOCH_2Ph$. The constancy of the ratio of benzaldehyde to *cis*-stilbene formed under aerobic conditions when H_2O_2 is utilized to produce activated BLM suggests a common activated BLM intermediate (A, in Scheme 3). In addition, the ratio of benzaldehyde to *trans*-stilbene varies as a function of O_2 concentration, and under anaerobic conditions only *trans*-stilbene is produced. These results are consistent with partitioning of a common intermediate (B). While $[Fe{\cdot}O]^{3+}$ can recycle *cis*-stilbene to catalytically produce products,

SCHEME 3

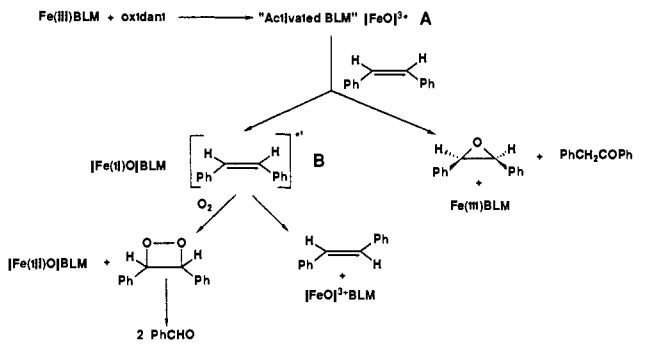

its ultimate fate has not been addressed.

These early studies indicate that "Fe·BLM" contains a rich chemistry awaiting exploitation. Because activated BLM has a reasonable half-life (minutes at 0 °C) and spectroscopic handles (UV–vis and EPR), the system is ripe for a detailed investigation of the mechanism of this nonheme iron–oxygen chemistry. It is reasonable to speculate that mechanisms will be elucidated analogous to those in P_{450} systems, with subtle variations dependent on the ligand arrangement, solvents, and the electronic configuration of the substrates (Scheme 4).[80]

C. Reactive Oxygen Radicals as Potential Mediators of Oxidative Damage to DNA

A number of investigators in the field showed that both HO· and $O_2^{\cdot-}$ are generated by Fe(II)·BLM and proposed that these active oxygen radical species may be responsible for degradation of DNA.[89-91] The Fe(II)·BLM-mediated production of HO· is based on ESR spin-trapping techniques using *tert*-butylnitrone and

SCHEME 4

HYDROXYLATIONS

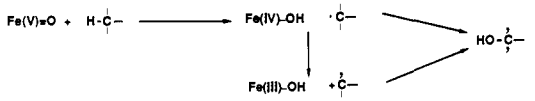

HETEROATOM OXIDATION

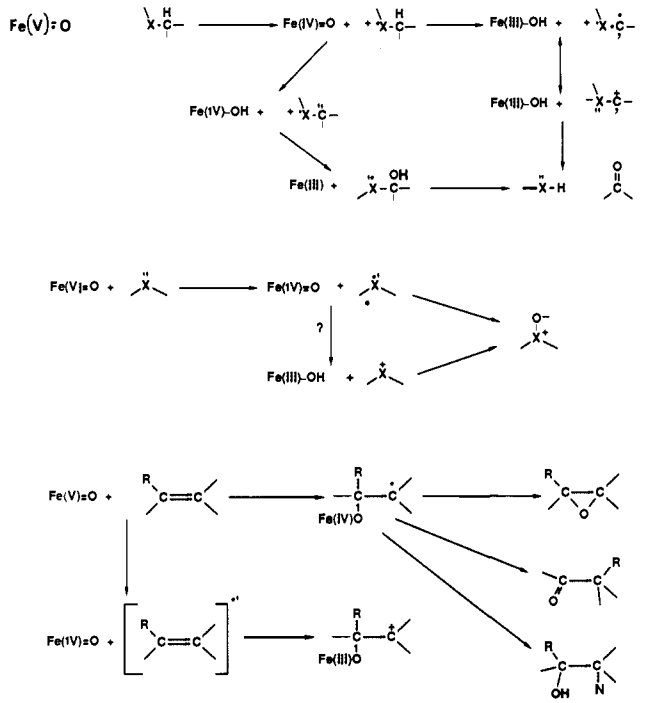

TABLE VIII

	redox, mV	relative spin concn of HO· by spin trapping
PYML 1[a]	0.03	18
PYML 4	0.11	71
PYML 6	0.16	97
BLM[194,28]	0.13	100

[a] Figure 7.

5,5-dimethyl-1-pyrroline *N*-oxide. (The many pitfalls associated with interpretation of spin-trapping experiments are reemphasized in a recent publication addressing the evidence for the existence of the peroxy radicals in the lipoxygenase system.[92]) In these studies, however, no effort was made to quantitate the amount of trapped adducts and to show that rate of radical production is kinetically competent to be involved in oxidative damage. While studies of Sugiura[28] showed that a reasonable correlation exists between the biological activity of a number of BLM analogues and the amount of spin-trapped HO· produced by these analogues in the presence of O_2, these observations probably reflect a correlation with the redox potential of Fe(II)·BLMs and Fe(II)/Fe(III) couple (measured by O_2 reduction) and may provide no information on the nature of the biologically active oxidant. In support of this notion are comparisons of the reduction potentials for a variety of man-made BLMs and their ability[89,92-94] to generate HO· (Table VIII, Figure 7). In fact, studies by Rodriguez and Hecht[96] indicated that *tert*-butylphenylnitrone does not inhibit DNA degradation as

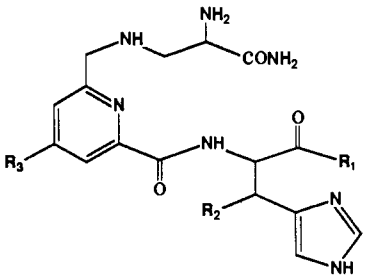

PYML-BLM

	R_1	R_2	R_3
PYML • 1	H	H	H
• 4	Bu^t	OBu^t	H
• 6	Bu^t	OBu^t	OMe

Figure 7. Structures of PYML-BLM.

measured by [^{3}]thymine production and that the amount of hydroxy radical spin-trapped adduct produced was about $^1/_{40}$ that observed with comparable amounts of Fe(II) and H_2O_2, a known HO· generator. In addition, studies with known hydroxy radical (HO·) scavengers, such as DMSO, indicated no effect on the rate of DNA degradation.

Finally, early studies of Lown and Joshua[90] indicated that superoxide dismutase (SOD) prevented BLM-mediated DNA degradation and were interpreted to indicate the active involvement of $O_2^{\cdot-}$ in the oxidative damage. More recent studies by Rodriguez and Hecht showed that a small molecule superoxide dismutase catalyst, tetrakis(4-*N*-methylpyridyl)porphineiron(III), had no effect on BLM-mediated DNA degradation. Furthermore, studies of Galvin et al.[97] showed that the inhibition of BLM-mediated degradation by SOD is unrelated to its effects on $O_2^{\cdot-}$ and that the previously observed inhibition more likely involves binding of the SOD to DNA.

The evidence described above, as well as the exquisite specificity of Fe(II)·BLM to mediate chemistry at the C4′ hydrogen of the deoxyribose moiety of a pyrimidine nucleotide adjacent to guanosine, mitigates against the involvement of freely diffusable active radical species such as HO· and $O_2^{\cdot-}$.

VI. Proposed Mechanisms for Product Production

Two types of monomeric products have been isolated and identified during Fe·BLM-mediated degradation of DNA: free nucleic acid bases and base propenals.[15,16,57] The base propenal formation requires O_2 in addition to that required to form activated BLM and is accompanied by DNA strand scission and phosphoglycolate termini production. The free base release requires no additional O_2 and is accompanied by production of an oxidatively damaged sugar in the intact DNA strand, which results in strand scission only in the presence of alkali (pH 12).[11] The proposed mechanistic pathway for production of base propenal and free base and the evidence that supports these proposed mech-

SCHEME 5

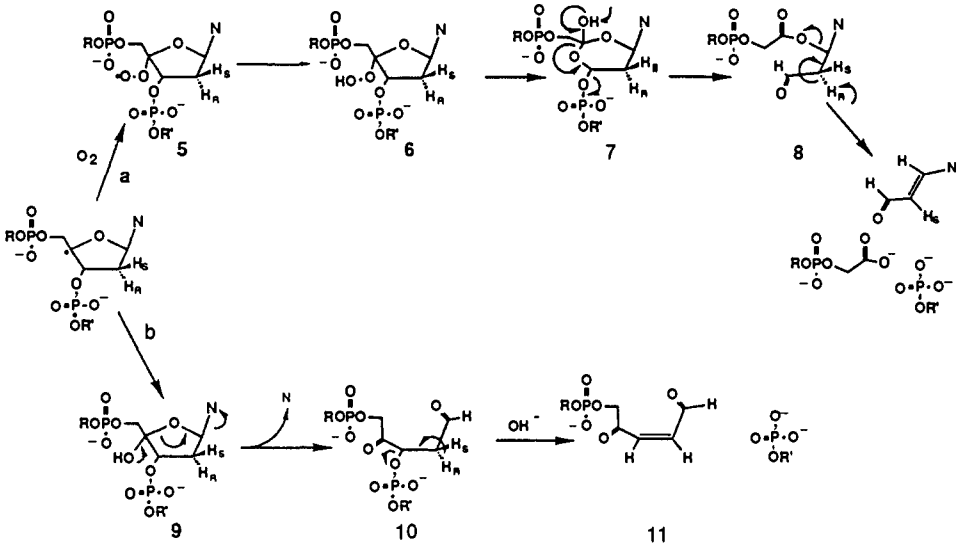

anisms are outlined in this section (Scheme 5).

A. Identification of Base Propenals and 3′-Phosphoglycolate Termini: Proposed Mechanism for Their Production

Through the extensive efforts to Burger et al.[16] it was established that the maldondialdehyde observed during BLM-mediated DNA degradation was produced from a product containing a nucleic acid base and a 3-carbon fragment derived from the deoxyribose ring. This monomeric product, base propenal, was ultimately isolated and unambiguously identified by GC–MS, in comparison with authentic material prepared chemically, through the efforts of Giloni et al.[15] In addition, they elegantly showed that each base propenal produced was accompanied by production of an equivalent amount of 3′-phosphoglycolate termini. The phosphoglycolate termini were identified by chemical (acid) and/or enzymatic (λ exonuclease) degradation, isolation of glycolic acid followed by derivatization, and GC–MS analysis. Recent studies by Uesugi et al. (1984)[98] using a hexamer, d(CGCGCG), and by Murugeson et al. (1985)[99] using a dodecamer, d(CGCTTTAAAGCG), and high-field NMR spectroscopy allowed direct observation of the 3′-phosphoglycolate oligomer, a point only inferred by the work of Giloni et al.[15]

The identification of base propenals and phosphoglycolate termini and the observation of Burger et al.[100] that O_2 in addition to that required to produce activated BLM was required to produce these products allowed Giloni et al.[15] to propose a reasonable mechanistic sequence to account for these results (Scheme 6). The observation of equivalent amounts of base propenal and phosphoglycolate termini requires 3′,4′ carbon–carbon bond scission of the deoxyribose ring. Giloni et al.[15] proposed, therefore, that activated BLM abstracts a hydrogen atom from the C4′ position to produce a 4′-carbon radical.

1. Evidence for 4′-Carbon–Hydrogen Bond Cleavage Associated with Monomeric Product Production

The key mechanistic evidence for 4′-hydrogen abstraction as a drug-mediated event has been our results using the model poly(dA-[4′-^{3}H]dU) as a substrate for Fe·BLM.[101,102] When poly(dA-[4′-^{3}H]dU) is degraded

SCHEME 6

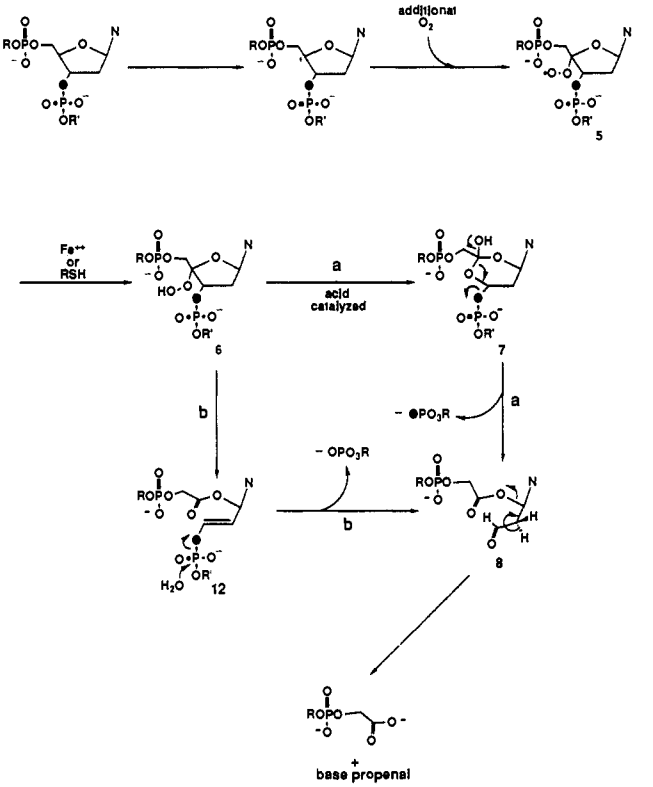

by activated BLM under a variety of conditions [Fe(II)·O_2·BLM or Fe(III)·H_2O_2·BLM], 50% ± 10% of the deoxyuridine residues were converted to uracil and uracilpropenal, paralleling observations made with DNA. Thus, poly(dAdU) appears to be a reasonable model for DNA. By manipulation of the concentration of O_2 in solution, the relative ratio of uracilpropenal to uracil could be varied between 0.03 for anaerobic activation (E, Table IX) and 7.0 for activation at 3 atm O_2 (D, Table IX). To establish if 4′-carbon–hydrogen bond cleavage was involved in production of either or both types of monomeric products, tritium selection effects on 4′-hydrogen abstraction, measured by the production of the product ^3H_2O, were measured under a variety of conditions (Table IX). Selection effects ranging from 10 to 12 were observed under various aerobic conditions at 4 °C (A–D, Table IX), and an

TABLE IX. Determination of the Primary Isotope Effect for the Abstraction of the 4′-Hydrogen from Poly(dA-[4′-^{3}H]dU) under Various Conditions[a]

reactn condn[b] (°C)	uracil, nmol	uracil propenal, nmol	reactn extent, fractn	^3H_2O, cpm	S,[c] cmp/nmol	κ_H/κ_T	κ_H/κ_T (adjusted)[d]
A (0)	6.6	8.3	0.35	451	416	7.8	10.9
A (0)	10.8	3.9	0.33	456	381	6.7	10.4
A (0)	8.7	9.5	0.50	459	459	9.5	12.5
D (0)	2.0	14.2	0.51	479	449	9.9	10.8
E (25)	17.2	0.4	0.58	758	466	6.5	7.2

[a] Uracil, uracil propenal, and ^3H_2O yields are expressed as amounts/50-μL reaction. [b] Reaction conditions: A, 10–20 mM poly(dAdU), 1.2 mM BLM, 1.1 mM ferrous sulfate, 10 mM sodium phosphate, pH 7.5, under normal atmosphere; D, same as A but under 3 atm O_2; E, 1.0–2.0 mM poly(dAdU), 0.6 mM BLM, 0.5 mM ferric ammonium sulfate, 8 mM H_2O_2, 10 mM sodium phosphate, pH 7.5, under anaerobic atmosphere. [c] S is the specific activity of unreacted [4′-^{3}H)deoxyuridine from the reaction. S_0 was determined individually for each experiment from a control reaction with BLM. The mean value of S_0 for these experiments was 195 cpm/nmol. [d] Best fit of data obtained by release of ^3H_2O and by determination of the specific activity of the unreacted starting material.

effect of 7.2 was observed for $Fe^{III}\cdot H_2O_2$ under anoxic conditions at 25 °C (E, Table IX).[102] These results strongly suggest that the formation of both uracil and uracilpropenal is the consequence of a rate-determining 4′-carbon–hydrogen bond cleavage and of an O_2-dependent partitioning of the intermediate produced by this cleavage (Scheme V). This hypothesis is consistent with the work of Giloni et al.[15] and Burger et al.[14] discussed above.

The significance of these findings lies in their unambiguous interpretation that 4′-hydrogen abstraction leads to both monomeric products, which we were unable to establish definitively by examining ^3H_2O, formation of product, as a function of extent of reaction. The reason for this is the ambiguity in correlating the amount of 4′-tritium released with the amount of uracilpropenal only or with the amount of both uracilpropenal and uracil.

To establish that cleavage of the 4′-carbon–hydrogen bond is associated with the production of both monomeric products, the specific activity of the starting material [4′-^{3}H]deoxyuridine in poly(dAdU) was examined as a function of extent of reaction (Figure 8). The extent of reaction was determined by production of either uracilpropenal alone (▲) or uracilpropenal and uracil (●). The results of a number of experiments (Figure 8) clearly establish that production of both products is associated with 4′-carbon–hydrogen bond cleavage. Furthermore, the relatively constant values for the selection effect under conditions yielding widely differing product ratios confirm our hypothesis that the processes resulting in uracil or uracilpropenal diverge from a common intermediate generated by hydrogen atom abstraction.

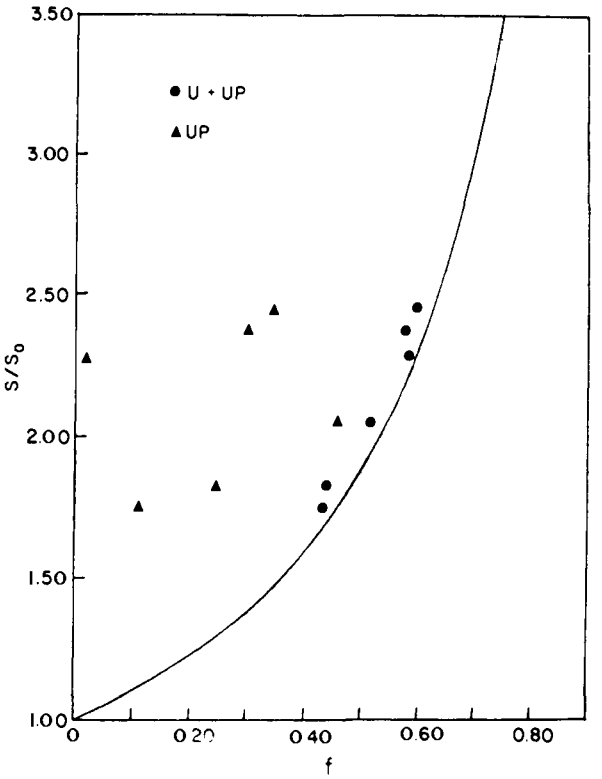

Figure 8. Specific activity (S/S_0) of unreacted deoxyuridine as a function of extent of reaction (f) for six representative bleomycin-poly(dA-[4′-^{3}H]dU) reactions.

2. Production of 4′-Peroxy Radicals and Their Fate

This 4′-radical intermediate, produced by hydrogen atom abstraction, under aerobic conditions would rapidly combine with O_2 to form a 4′-peroxy radical. Giloni et al.[15] proposed that this peroxy radical is reduced by an as "yet unidentified reductant" to produce the 4′-hydroperoxide species. This species was then proposed to collapse by pathway a (Scheme 6) in a facile reaction to produce 8, which would be the direct precursor to the products. Alternatively, they suggested that collapse of the 4′-hydroperoxide might proceed by pathway b[104] (Scheme 6), in which a 2′-hydrogen is removed, triggering 3′,4′ carbon–carbon bond cleavage and producing enol phosphate **12**. Attack of H_2O on the phosphate moiety of the enol phosphate would ultimately produce the observed products.

This latter mechanism is chemically unappealing, as the hydrogen attached to C2′ of the deoxyribose moiety has a $pk_a \sim 30$ and hence would not readily be removed. Recent studies of Ajmera et al.[105] using 3′-[^{18}O]-labeled poly(dAdT) showed that this mechanism is indeed incorrect. As indicated in Scheme 6, pathway a predicts that [^{18}O] would be found in P_i after degradation of the polymer, while pathway b predicts that [^{18}O] would be found in the base propenal. Using ^{31}P NMR spectroscopy Ajmera et al.[105] showed that all of the ^{18}O, within experimental errors, is found in the P_i.

Pathway a, however, requires serious consideration, and each step will be discussed in some detail. As outlined in the previous section, use of [4′-^{3}H]-labeled DNA models has allowed unequivocal support for C4′ carbon–hydrogen bond cleavage.[101,102] The second step addition of O_2 to the radical R· to form a peroxy radical ROO· is extremely fast and is probably diffusion controlled in most cases (10^9 M^{-1} s^{-1}).[103]

EPR spectroscopic methods established that peroxy radicals have g values (line positions) in the range of

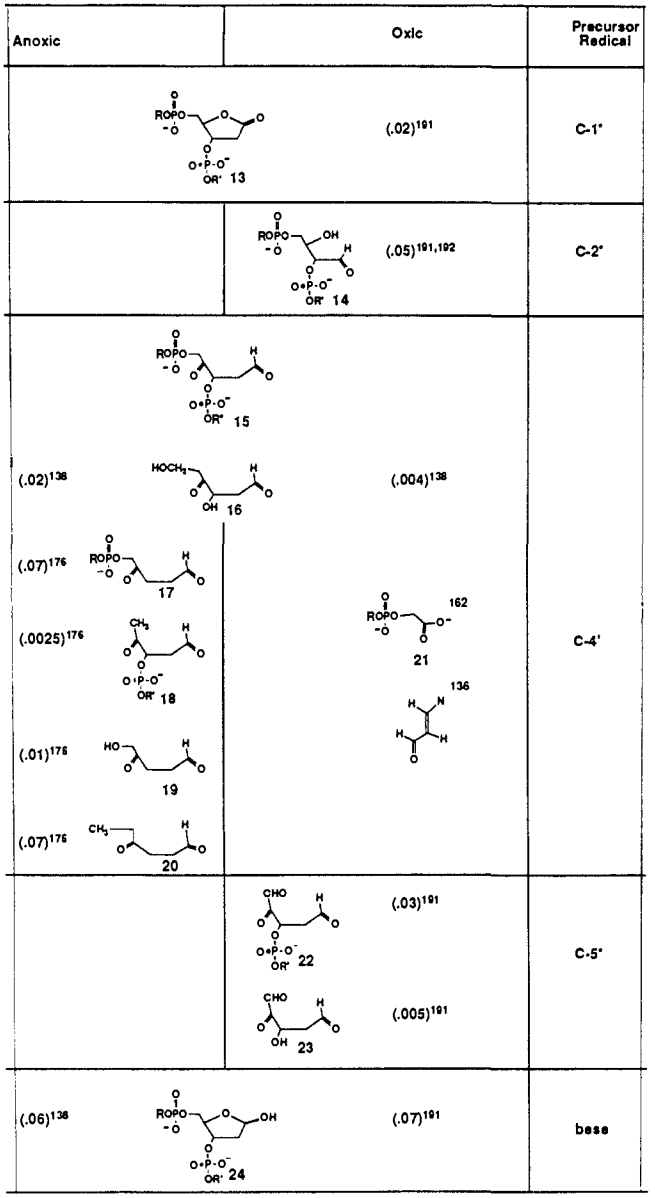

Figure 9. Alterations at the sugar moiety in the γ-radiolysis of DNA in anoxic and oxic solutions and site of precursor radicals. Compounds to left of center are produced solely under anoxic conditions; those to the right of center are produced solely under oxic conditions. Compounds in the center are produced under anoxic and oxic conditions. The number in parentheses refer to G values.

2.014–2.019, making them easily distinguishable from organic radicals, which have g values near that of the free electron, $g = 2.0023$.[181] While no direct evidence for peroxy radical production exists in the BLM system, using EPR rapid flow methods Bothe et al.[106,107] recently reported observation of peroxy radicals studying γ-radiolysis of poly(U). The location of the poly(U) peroxy radicals, base or sugar, has not been unambiguously identified.

The fate of peroxy radicals has been studied extensively[103,108] (for recent reviews). Von Sonntag and coworkers proposed, from their extensive γ-radiolysis studies on DNA models, that many of the products observed (Figure 9) can be accounted for by multistep pathways involving the initial self-condensation of two tertiary peroxy radicals to form tetraoxides (eq 2). This

$$2\text{ROO}\cdot \rightarrow \text{ROOOOR} \rightarrow 2\text{RO}\cdot + \text{O}_2 \qquad (2)$$

$$2\text{RO}\cdot \rightarrow \text{ROOR}$$

dimerization reaction would appear to be sterically hindered with DNA-like substrates and, in addition, studies summarized by Ingold[103] suggest that proposed reactions of tetraoxides, made from dimerization of tertiary peroxides, are slow ($0.1–6.0 \times 10^4$ M^{-1} s^{-1}) due to the high activation energy for the decomposition of the tertiary tetraoxides.

These problems aside, however, the role of tetraoxides is supported by studies of Bothe et al.[106] Their results have been interpreted to indicate that poly(U) peroxy radicals are involved in the rate-determining step of strand scission. Furthermore, they observed that dithiothreitol (DTT) inhibits strand scission, and postulated that DTT reacts with ·OOR to form HOOR, preventing breakage. Since these studies were done on single-stranded poly(U) and the location of the peroxy radicals could be the nucleic acid base, the relevance of these studies to BLM, while interesting to consider, still remains to be established.

Peroxy radicals can enter into a wide variety of reactions other than formation of tetraoxides and, in the case of DNA peroxy radicals, these reactions may be limited to hydrogen atom abstractions. These oxidations are only likely to proceed if the bond that is formed (ROOH) (90 kcal/mol) is at least as strong as that which is broken (X ~ H). The resonance weakened O–H and S–H bonds of (FeOH) or reductants such as a thiol may be readily abstractable hydrogen atoms.[108] Alternatively, ROO· can undergo chain termination by reduction via transition-metal oxidations (eq 3). This reaction is as fast as H· abstraction from efficient amines or phenols, $\sim 2 \times 10^5$ M^{-1} s^{-1}.[103]

$$\text{ROO}\cdot + \text{Mn(II)} \rightarrow \text{ROO}^- + \text{Mn(III)} \qquad (3)$$

Therefore, it seems reasonable that the 4′-peroxide could be generated by either H· abstraction, perhaps from FeOH or RSH if present for catalysis. A Fe(II)·BLM-mediated reduction would seem unlikely due to steric accessibility. The proposed reduction of the peroxy radical to the hydroperoxide appears to be chemically reasonable.

3. Conversion of 4′-Hydroperoxide to Base Propenal and 3′-Phosphoglycolate Termini

a. **Criegee-Type Rearrangement.** Conversion of the 4′-peroxide to 8 has been proposed to occur via an ionic, acid-catalyzed heterolytic cleavage of the O–O bond of the peroxide (eq 4).[109–112]

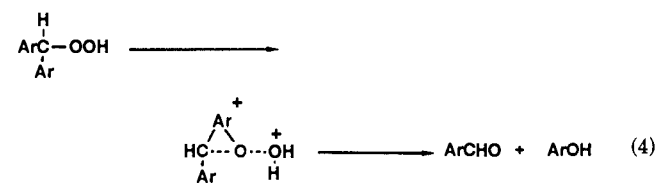

(4)

In general, the rates of this type of reaction were found to be more rapid with migrating groups that stabilize the developing positive charge in the transition state. The migratory aptitudes were determined to be aryl > vinyl > H > 3° alkyl > 2° alkyl > 1° alkyl. This proposed mechanism applied to the 4′-OOH intermediate in the BLM-catalyzed reaction would thus require an alternative to acid catalysis and, in addition, would be on the "slow" end of the reaction scale because of the secondary alkyl nature of the proposed migrating

SCHEME 7

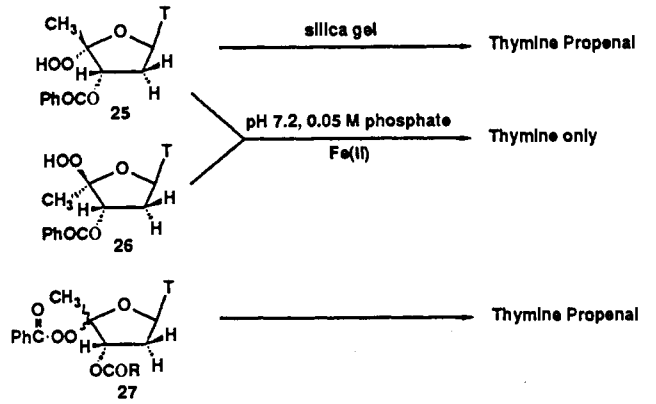

species. Instead of a proton catalyzing the reaction, the Fe·BLM intermediate could act as a Lewis acid.[113] The proposed role for iron in this reaction has precedence in enzymatic systems as well. The protocatechuate dioxygenase[114,115] is an example, which is given in eq 5.

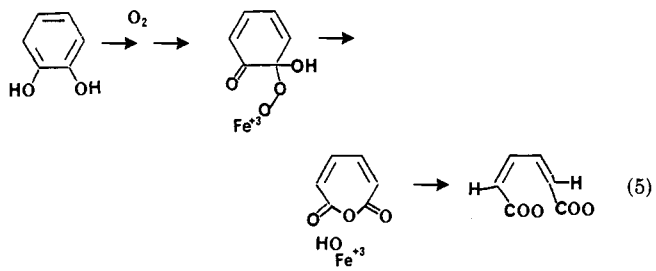

The high-spin Fe(III), which does not undergo redox chemistry during the conversion of catechol to *cis,cis*-muconate, is proposed to act as a Lewis acid in the rearrangement of the peroxide to form products. Quite interestingly, no exchange with solvent occurs during this rearrangement, as evidenced by the 1 equiv of oxygen from $^{18}O_2$ found in each of the carboxylates of the *cis,cis*-muconate produced.

b. Model Studies. A recent model system for the proposed rearrangement in the BLM case was examined by Saito et al.[116,193] These workers prepared the epimeric mixture of 3′-*O*-benzoyl-5′-deoxy-4′-hydroperoxythymidines **25, 26** (Scheme 7) by reaction of H_2O_2 with 1-(3-*O*-benzoyl-2,5-dideoxy-β-D-glyceropenta-4-enefuranosylthymidine. Attempts to isolate **25** via silica gel chromatography resulted in its decomposition to thymine propenal. If the mixture of epimers **25, 26** were incubated at pH 7.2 in the presence of iron in aqueous solution (typical conditions for BLM-mediated DNA degradation), only thymine was observed. If the peroxybenzoate ester of the epimeric mixture was examined in CH_3CN at 60 °C, thyminepropenal was the major product isolated. Observation of the collapse of **25** to thyminepropenal on silica gel is potentially an excellent model for the proposed BLM chemistry (Scheme 7). However, the possibility must be considered that the 3′-benzoyl group of **25** migrates to the terminal oxygen of the 4′-peroxide (this can only happen with this epimer because of the stereochemistry) to form an acyl peroxide. [Note added in proof: Decomposition of the 4′-hydroperoxide **25**, which has both oxygens of the peroxy group labeled with ^{18}O, resulted in 96% incorporation of a single atom of ^{18}O into the carboxylate group of the benzoic acid product. This result strongly suggests facile intramolecular transfer of the benzoyl moiety from the 3′-oxygen to the terminal oxygen of the 4′-hydroperoxide (McGall et al., unpublished results).] This compound, as with the peroxybenzoate **27**, would be expected to undergo facile heterolytic cleavage of the O–O bond by a Criegee-type rearrangement to produce thyminepropenal.[117] The acid-catalyzed decomposition of **25**, or a similar nucleoside in which the 3′-position is blocked with a group not capable of undergoing migration, has not been examined. If conditions can be established where thyminepropenal is observed, then the details of the reaction—identification of products, intermediates, and mechanism using ^{18}O-labeled peroxide—would be of interest to investigate.

4. $^{18}O_2$ Pulse–Chase Experiments: Source of "O" in the Oxidized Products Produced

From the model chemistry and enzymatic systems discussed above, a mechanism for the acid-catalyzed decomposition of peroxide in the BLM system can be proposed. In this model, the peroxide is complexed with the active BLM, and the "Fe" is proposed to play a role as a Lewis acid to facilitate heterolytic bond cleavage. In the tight ion pair formed, the carbonium ion is stabilized by unpaired electrons on both oxygens, and migration of the secondary alkyl carbon in preference to the primary alkyl carbon is proposed because of migratory aptitudes previously elucidated in acid-catalyzed peroxide rearrangement reactions. The ion pair then collapses to add an "H_2O equivalent" derived initially from O_2 to the 4′-carbonium ion without prior exchange with solvent. This intermediate **7** would then decompose in several steps to produce 3′-phosphoglycolate ends and thyminepropenal, each containing one ^{18}O from the $^{18}O_2$ (Schemes 5 and 6).

Recent studies from our laboratory[118] designed experimental protocols allowing us to test this hypothesis. The kinetics of BLM-mediated degradation of DNA (section VA) allow a distinction to be made between O_2 (O_2 pulse) required to produce activated BLM and the additional O_2 (O_2 chase) essential for production of base propenal.

The mechanism in Schemes 5 and 6 predicts that O_2 in the 3′-phosphoglycolate-modified oligonucleotides is derived from O_2 in the chase. To test this hypothesis, DNA was treated with activated BLM, and the reaction mixtures were then treated with P1 nuclease and alkaline phosphatase. This treatment released free glycolic acid from 3′-phosphoglycolate termini, which was isolated by anion-exchange chromatography and converted to a di-TMS derivative for analysis by GC–MS.

The mass spectrum of glycolic acid isolated from reactions carried out under an $^{18}O_2$ atmosphere shows that a single atom of ^{18}O is incorporated, at levels between 90 and 98%, into the carboxylate group of this molecule. This was found to be the case regardless of whether bleomycin was first activated with Fe(II) and $^{18}O_2$, Fe(II) and $^{16}O_2$ prior to the introduction of DNA and excess $^{18}O_2$, or with Fe(III) and H_2O_2 in the presence of DNA and $^{18}O_2$. Activation of the drug with $^{18}O_2$ and Fe(II) prior to reaction with DNA under $^{16}O_2$ did not result in significant amounts of ^{18}O in the product (Table X). These results demonstrate that the oxygen incorporated at deoxyribose C4′ derives primarily from the "second" O_2 requirement and not the O_2 involved

TABLE X. Percent Incorporation of ^{18}O into the Glycolic Acid Obtained from the Degradation Products of Calf Thymus DNA with Fe-bleomycin

activation pulse	reactn chase	1-(^{18}O)glycolic acid, %
$^{16}O_2$/Fe(II)	$^{18}O_2$	89.5
$^{18}O_2$/Fe(II)	$^{16}O_2$	3.5
$H_2{}^{16}O_2$/Fe(III)	$^{18}O_2$	94.2

in drug activation (Scheme 5). This supports the hypothesis that strand scission is preceded by the addition of molecular oxygen to a deoxyribose C4′ radical resulting from the attack of activated bleomycin. Similar results were obtained using poly(dAdU), d(CGCGCG), and calf thymus DNA.

Determination of the source of oxygen in the base propenals has proven to be more complicated than the glycolate studies outlined above. Aldehydes and ketones can undergo rapid hydration, which can result in washout of ^{18}O label and necessitate the use of a trap to prevent such washout.[119] The mechanism proposed in Scheme 5 also predicts that one atom of oxygen derived from O_2 in the chase should be found in base propenal. We also recently developed a method to rapidly isolate base propenals from the reaction mixture. These compounds were reduced with $NaBH_4$ and ultimately derivatized with *N,O*-bis(trimethylsilyl)-2,2,2-trifluoroacetamide (BSTFA):CH_3CN (1:1) and 1% trimethylsilyl chloride (TMSC) for analysis by GC–MS. This method resulted in excellent recoveries of derivatized thyminepropenal (85%), adeninepropenal, and cytosinepropenal. To determine the source of oxygen in the thyminepropenal, an initial experiment was attempted by incubation of Fe(II)·$^{18}O_2$·BLM, $^{18}O_2$, and poly(dAdT) at pH 7.5 for 15 min at 0 °C. The thymine propenal was then isolated and analyzed by GC–MS. The results shown in Figure 10 indicated that no ^{18}O oxygen was present in product.

To determine if the lack of ^{18}O in thyminepropenal was due to exchange from product, a control experiment was run. [^{18}O]Thyminepropenal was prepared and incubated in the presence of Fe(II)·O_2·BLM for 15 min at 0 °C. At the end of the reaction, the thyminepropenal was analyzed in a fashion identical with the experiment. To our surprise, the GC–MS showed almost no washout of ^{18}O (~10%) from the thyminepropenal! The fact that no ^{18}O from $^{18}O_2$ is observed in the base propenal in the experiment, for the mechanism in Scheme 6 to be valid, therefore requires ^{18}O exchange from a precursor to the final product such as compound 8, Scheme 6. In analogy with CH_3CHO, exchange is expected to occur rapidly from such an intermediate.[119] Rapid trapping of the proposed intermediate will, therefore, be required to establish the stoichiometric transfer of ^{18}O from the chase $^{18}O_2$ into the base propenal precursor.

5. Evidence for a "Stable" Intermediate as a Precursor to Base Propenal and 3′-Phosphoglycolate Termini

In late 1986, Burger et al.[120] reported that Fe(II)·O_2·BLM-mediated cleavage of DNA could be resolved into two kinetic components. The rate of strand scission, monitored with viscometric and fluorometric methods, was determined to have a half-life of 2.5–5.0 min at 4 °C, while the rate of base propenal production under identical conditions was reported to have a half-life of 40 min. These results are consistent with the proposal in Scheme 5, where strand scission produces 5′-phosphate termini and 8, which can, subsequent to removal of the 2′-*pro-R* hydrogen, be converted to base propenal. Intermediate 8 would be expected to rapidly exchange the oxygen of its aldehyde moiety with solvent and could therefore account for substoichiometric (8%) ^{18}O observed in the thyminepropenal from $^{18}O_2$ chase experiments.

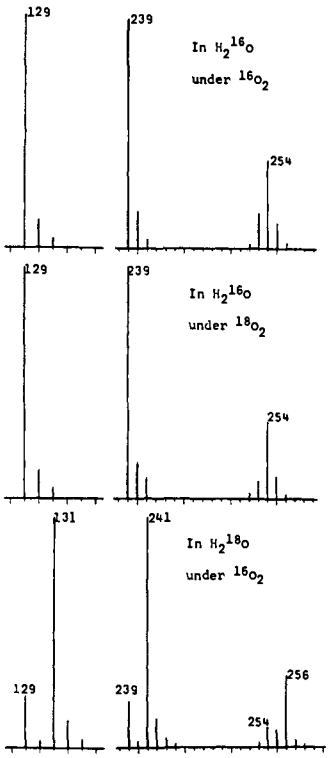

Figure 10. MS Derivatized [^{18}O]thyminepropenal.

However, Burger et al.[120] performed an additional experiment, which is inconsistent with the mechanism proposed in Scheme 5. These workers incubated DNA, [^3H]-labeled with 1′,2′-5-thymidine with Fe(II)·O_2·BLM under conditions analogous to those in which they measured strand scission and measured the rate of ^3H_2O production. [Neither the distribution of [^3H] between the 1′-, 5-, and 2′-*pro-R* and *pro-S* positions, nor the specific activity of [^3H] in the thymidine in the DNA or product thyminepropenal were reported. These numbers are required for quantitation of the observed results. In addition, the amount of thymine was not reported, and previous studies from our laboratory determined that small amounts of ^3H_2O production from [2′-*pro-R*-^3H]poly(dAdU) (probably via an enolization reaction) accompany base release.] They observed that the $t_{1/2}$ of ^3H_2O production was 1.8 min, comparable with that observed with strand scission and much slower than the rate of base propenal production. The mechanism in Scheme 5 would predict that ^3H_2O production should occur at a rate less than or equal to base propenal production, depending on the selection effect on 2′-C–H bond scission.

On the basis of their studies, Burger et al. proposed the following mechanism for conversion of the 4′-hydroperoxide to final products (Scheme 8). A Criegee-type rearrangement results in production of **28**. Removal of the 2′-*pro-R* hydrogen of **28** (^3H_2O production) is proposed to be required for strand scission

SCHEME 8

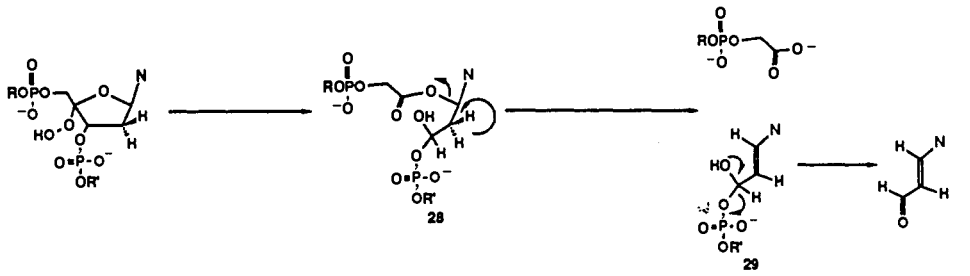

and production of the 3′-phosphoglycolate ends. This proposal is chemically unappealing for several reasons. First, the 2′-hydrogen of **28** is unactivated, having a very high pk_a. Second, this mechanism requires that collapse of the tetrahedral intermediate $O_3POC(OH)HR$ occurs with a half-life of 40 min. Rates of dehydration of hydrated aldehydes under neutral conditions at 0 °C in the worst case occur with $k = 0.001\ s^{-1}$, that is, a $t_{1/2} \sim 11$ min. Since OPO_3R should be a better leaving group than OH, if **28** (Scheme 8) were the intermediate, then it should decompose with a much shorter half-life than that observed.

Careful examination of the experiments of Burger et al. allows an alternative interpretation to account for the observed rapid rate of ^3H_2O production. In all of their experiments, the reactions were stopped by addition of 1 M salt to facilitate DNA precipitation, followed by an increase in both buffer concentration and salt concentration when analyzing for ^3H_2O production by bulb-to-bulb distillation. It is possible that, at these high buffer concentrations and ionic strengths, that enolization of the proposed intermediate is accelerated (eq 6) and causes rapid washout of ^3H from both 2′-

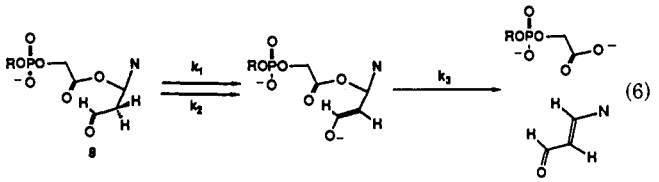

(6)

pro-R and *-pro-S* positions. Precendent for such an enolization mechanism on a similar system was observed in the inactivation of *Escherichia coli* ribonucleotide reductase by 2′-chloro-2′-deoxyuridine 5′-diphosphate (ClUDP) (eq 7).[121] We have shown, using

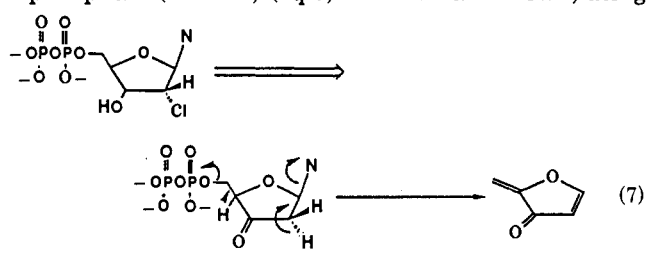

(7)

[2′-^{3}H]ClUDP (0.05 M, Hepes pH 7.5), that rapid enolization precedes base release. Whether this enolization mechanism can account for the results of Burger et al. is presently being investigated with [2′-*pro-R*-^{3}H]DNAs and [2′-*pro-S*-^{3}H]DNAs ± 1 M salt. Results from these experiments are critical to the proposal outlined in Scheme 5.

B. Proposed Mechanism for Base Release

The isotope effect data, discussed in detail in this section (A1), clearly indicate that the rate-determining step in BLM-mediated base release from DNA is 4′-C–H bond cleavage of the deoxyribose sugar moiety. The isotope effect is large regardless of whether BLM is activated by Fe(II) and O_2 or $Fe^{III}\cdot H_2O_2$. These results allowed us to propose the working hypothesis for base release shown in Scheme 9 (a and b). In Scheme 9a the activated BLM mediates a hydrogen atom abstraction from the C4′ carbon to produce the 4′-carbon radical. The 4′-radical may then undergo a radical rebound mechanism, in analogy with proposals of Groves and co-workers for cyt P_{450} systems,[59,122] to produce **30**. Alternatively (Scheme 9b), the radical could be oxidized by "Fe^{III}·OH" to produce a C4′ carbonium ion, which could then add H_2O to produce the same intermediate **30**. This intermediate **30** can then collapse via a one- or two-step sequence to produce **31** and free base. The modified sugar residue **31** in the presence of OH^- could undergo strand scission to produce 5′-phosphate termini.

SCHEME 9

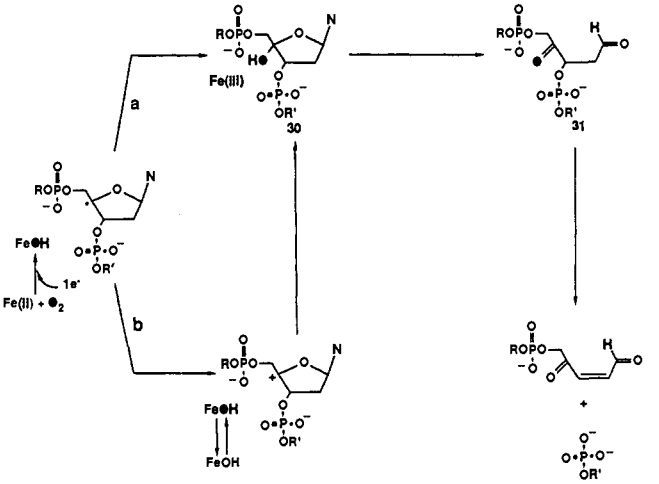

1. Identification of the Oxidized Sugar Accompanying Base Release

This proposal makes a number of predictions that we have tested experimentally. The first is the identity of the structure of the oxidized sugar accompanying monomeric base production.[123]

Bleomycin (BLM) in the presence of Fe(III) and H_2O_2 under anaerobic conditions catalyzes the degradation of DNA to produce free base and an intact DNA backbone, which undergoes scission only after treatment with hydroxide (Scheme 9). To simplify identification of the modified carbohydrate moiety remaining subsequent to base release, hexamer d(CGCGCG) was incubated with $Fe^{III}\cdot H_2O_2$ under anaerobic conditions and shown to produce cytosine and a new product, which was isolated by reversed-phase high-pressure

SCHEME 10

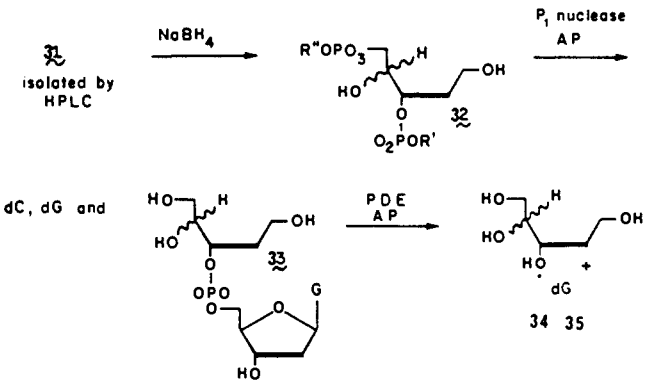

liquid chromatography (HPLC). The new product was stabilized by NaB^3H_4 reduction, purified, and degraded with P_1 nuclease and alkaline phosphatase to produce a mixture of diastereomers—2-deoxy-L-*threo*-pentitol (**34**) and 2-deoxy-D-*erythro*-pentitol (**35**) attached through their 3′-hydroxyl to the 5′-position of 5′-dGMP (**33**; Scheme 10). The 2-deoxy-D-*erythro*-pentitol-5′-GMP (**33**) comigrated in three HPLC systems with an authentic sample prepared chemically. The mixture of diastereomers was then further degraded with snake venom phosphodiesterase to produce GMP and the reduced sugars **34** and **35**. Compounds **34** and **35** comigrated in two TLC systems with these compounds prepared by independent syntheses. In addition, **34** and **35** were unambiguously identified by GC–MS subsequent to derivatization with a 1:1 mixture of BSTFA:CH_3CN with 1% trimethylsilyl chloride at 100 °C for 30 min. Comparison of the fragmentation patterns (Figure 11) of NaB^2H_4 with $NaBH_4$-reduced sugars not only established the identification of the sugars but also the location of deuterium at C1 and C4 (Rabow et al., unpublished results).

Similar products were also isolated by using d(CGCGCG), Fe(II), O_2, and BLM in addition to the other expected products from the O_2-dependent base propenal pathway. Therefore, activated BLM generated either by Fe(II), O_2, and reductant or $Fe^{III}{\cdot}H_2O_2$ (anaerobic) produced free base and a DNA backbone whose structure is consistent with the hypothesis we put forth[101,102] that base release is mediated by 4′-hydrogen atom abstraction followed by 4′-hydroxylation. Very recently, similar studies using poly(dGdC) and calf thymus DNA identified **34** and **35** (subsequent to analysis in Scheme 10) as the oxidized sugars produced accompanying base release.

Sugiyama et al. (1985),[124] in an effort to define the structure of the damaged sugar accompanying base release, recently did a similar experiment using a dodecamer, d(CGCTTTAAAGCG), and OH^- rather than $NaBH_4$ as a trapping agent. Hydroxide trapping is proposed to occur as indicated in Figure 12. While Sugiyama et al. reported isolation of a product from BLM-mediated degradation of the dodecamer that comigrated with an authentic sample of **36**, no quantitation of the product produced or its correlation with base release was reported.

The proposed mechanism for base release and results of Sugiyama et al.[124] suggest that treatment of DNA damaged by BLM with OH^- should result in the production of a 3′-phosphate-modified terminus. Gel electrophoresis techniques using **36** (Figure 12) and the

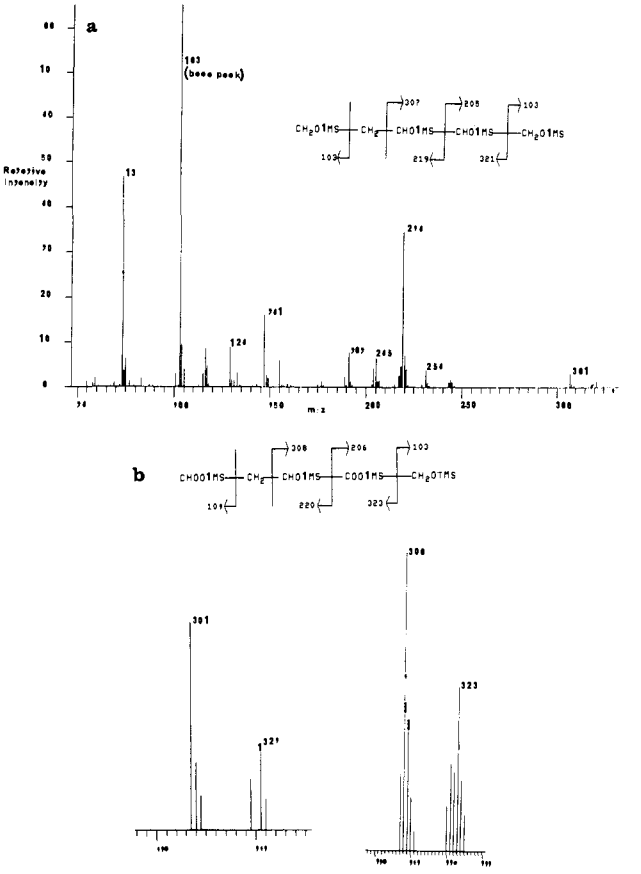

Figure 11. (a) Mass spectrum of the TMS derivative of the chemical standard 2-deoxy-D-*erythro*-pentitol. (b) Comparative partial mass spectra, chemical standard vs. bleomycin reaction product.

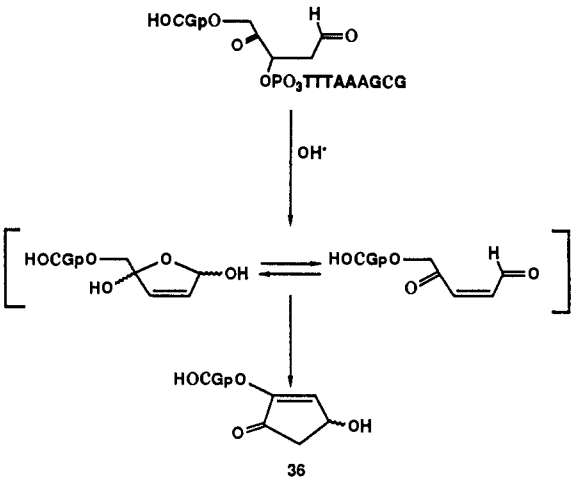

Figure 12. Trapping with OH^- of modified carbohydrate accompanying base release.

corresponding oligomers containing 3′-phosphate and 3′-OH termini should establish if a distinction can be made between these three termini. The original scheme predicts that these termini should also be observed in DNA restriction fragments, and electrophoresis methods should be examined more closely to look for these products.

2. $^{18}O_2$ Pulse–Chase Experiments: Attempts To Define the Source of O in the Oxidized Carbohydrate Moiety Accompanying Base Release

The mechanism proposed in pathway a (Scheme 9) to account for the products observed predicts that the

oxygen of the ketone at C4′ is derived from the O_2 (pulse) required to produce activated BLM. To test this hypothesis we incubated d(CGCGCG) under conditions of limiting $^{18}O_2$; that is, enough $^{18}O_2$ was present to produce only the activated BLM, and hence pathway b of Scheme 5 predominated over pathway a. Subsequent to 15-min reaction at 0 °C, the damaged oligomer (**31**) (Scheme 10) was isolated by HPLC and immediately reduced with $NaBH_4$ to minimize exchange of ^{18}O from the 4′-ketone, as well as to submit the oligonucleotide to the workup previously described (Scheme 10). Isolation and derivatization of the diastereomers of pentitols, followed by GC–MS analysis, indicated no [^{18}O]pentitol produced. We had hoped that **31** would exist predominantly as the hydrate (eq 8) and would

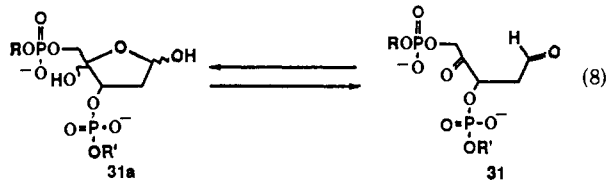

(8)

greatly slow down ^{18}O washout from ketone, allowing isolation of the ketone oligonucleotide by HPLC prior to trapping by reduction. Lack of ^{18}O in the trapped pentitols is consistent with the proposed mechanism only if rapid washout has occurred. This experiment is being repeated in the presence of $NaBH_4$ in an attempt to trap the ketone as rapidly as it is produced, before exchange can occur.

Pathway b (Scheme 9) proposes that Fe^{III}·OH can oxidize the C4′ radical to a stabilized C4′ oxonium ion. Addition of H_2O results in production of the same intermediate **30** as predicted from pathway a. However, in this case the source of the C4′-OH could be solvent or H_2O derived originally from $^{18}O_2$ gas and reduced to H_2O during the sequence of events leading to base release. If the H_2O equivalent bound to Fe(III) can exchange with solvent or the Fe^{III}·OH equivalent is no longer juxtaposed with the 4′-oxonium ion, then the oxygen in the 4′-ketone (**31**) will ultimately be derived from solvent and not O_2 gas. If $^{18}O_2$ is ultimately trapped in 4′-ketone, a distinction between the oxygen rebound mechanism and oxidation, H_2O addition without solvent exchange mechanism cannot be made.

VII. Co(III)·BLM

BLM was shown by a number of investigators to form exchange-inert complexes with cobalt.[21,31,125–130] Because of this property and BLM's ability to localize specifically in tumor cells in man and in other animals, it has been investigated as a carrier of ^{57}Co (a γ-emitting metal ion) and as a diagnostic tool to locate tumor cells.[125,131] Unfortunately, the $t_{1/2}$ of ^{57}Co is 270 days rather than a desired several hours or days, which would be required for a clinically useful diagnostic tool.

Chang and Meares[132] and Meares et al.[133] also made the intriguing observation that Co(III)·BLM in the presence of light induces DNA strand scission. This observation, and reports that Co(III)·polyamine complexes can undergo photoreduction,[134,135] allowed Barton and co-workers[5] to prepare chiral phenanthroline·Co(III) complexes that recognize different local structures of DNA producing photoreactive site specific DNA cleaving reagents. The chemistry and mechanism(s) of light-induced oxidative damage are thus of considerable interest.

TABLE XI. Spectral Properties of Co(III)·BLMs

X^-	color	λ_{max}
HOO·Co(III)·BLM	green	594[a]
H_2O·Co(III)·BLM	golden brown	544
formate·Co(III)·BLM	brown	560
Co(III)·BLM	orange	520
SCN·Co(III)·BLM	burgundy	552

[a] The structure has been proposed by Albertini and Garnier-Suillerot[26] to be a μ-peroxo Co(III) complex.

SCHEME 11

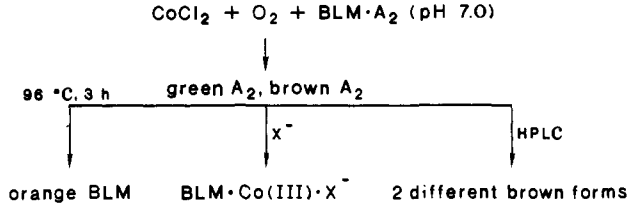

A. Structure of Co(III)·BLMs

Extensive EPR studies of Sugiura[27] with BLM and a number of its analogues indicated that Co(II) forms a low spin 1:1 complex with BLM, which possesses square-pyrimidal geometry and an axial "N" donor (Table I). Addition of O_2 to the solution is claimed to produce a monomeric low-spin [Co(II)] dioxygen adduct. EPR studies using iso-, dep-, and deamido-BLM analogues (Table I) have been interpreted to indicate that the α-amino nitrogen of the β-aminoalanine portion of BLM is the fifth axial ligand (Figure 3). Since Co(III)·BLMs are produced from $CoCl_2$ and BLM in the presence of O_2, proposed structures of these precursors have strongly influenced thinking about the structures of the Co(III)·BLM derivatives isolated.

A number of laboratories prepared Co(III)·BLMs from Co(II), O_2, and BLM; however, it was not until recently that the complex mixture of products produced were separated and partially characterized[31,124,127,130] (Scheme 11, Table XI). The Co(III)·BLMs are isolable with CM-Sephadex (ammonium formate elution) followed by reversed-phase HPLC. Recently Chang et al.[127] characterized a number of these compounds by fast atom bombardment (FAB) mass spectrometry and concluded that the green and brown Co(III)·BLMs are octahedral with one external ligand, the others being derived from BLM. The green complex is proposed to have hydroperoxide (OOH^-) as a ligand, whereas the brown complexes are proposed to have H_2O or formate as ligands. The "orange" BLM is thought to have all six ligands provided by BLM. Chang and Meares showed that "brown" BLMs bind to DNA with K_{assn} = 1.3–5 × 10^7 M and possess good DNA cleaving ability. These results contrast with studies on the orange BLMs, which have lower affinity for DNA (K_{assn} = 1.5 × 10^5 M) and have lower nicking capacity. Thus, recent attention has been focused on the green and brown Co·BLMs.

B. Products Produced and Proposed Mechanism of Their Production

Studies by Wensel et al.[133] on [^{32}P]-end-labeled DNA and brown or green Co(III)·BLM indicate that the

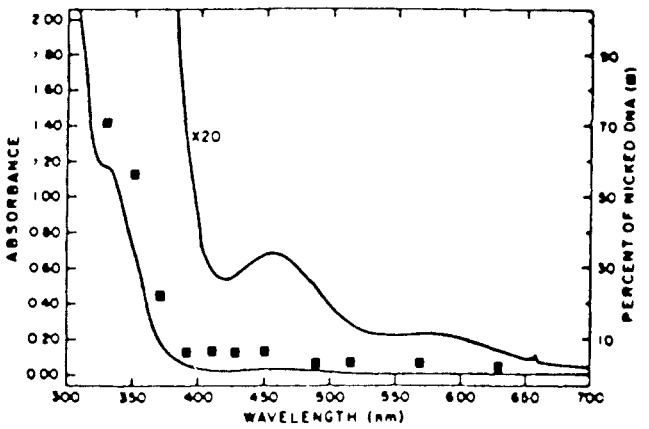

Figure 13. Action spectrum of Co(III)·BLMs: DNA nicking by cobalt-bleomycin compared with the absorption spectrum of cobalt-bleomycin.

cleavage patterns are very similar to those observed with Fe(II)·BLM and suggest that 3′-phosphoglycolate-modified ends are produced. In addition, both Co(III) ($h\nu$) and Fe(II)·BLMs give the same alkali-labile sites, resulting in 3′-phosphate-modified ends. While Chang and Meares[132] were able to detect free base release (thymine), attempts to detect base propenals with the malondialdehyde assay failed. No O_2 requirement for strand scission and base release was apparent, and Co(III)·BLM did not appear to undergo self-inactivation during its degradation of DNA.

Of critical importance in defining the chemistry of Co(III)·BLM-mediated DNA strand scission is its action spectrum. Chang and Meares[132] showed that maximum strand scission is correlated with light absorption at 330 nm, a charge-transfer band (Figure 13). Previous studies from Adamson's laboratory[134,135] showed that Co(III) complexes undergo two types of light-induced reactions: photoreduction and photosubstitution. Irradiation of the charge-transfer band tends to produce photoreduction products Co(II) and an oxidized ligand. Whether Co(II) and an oxidized ligand (pyrimidine? bithiazole?) is produced during $h\nu$-mediated DNA degradation remains to be established. It is possible that the oxidized ligand could mediate H atom abstraction from the deoxyribose moiety of DNA.

The similar specificity of cleavage observed for Co(III)·BLMs in comparison with Fe·BLMs suggests that binding and/or chemistry probably occurs within the minor groove of B-form DNA. [^{3}H]DNA models could therefore be utilized to establish if 1′- and/or 4′-carbon–hydrogen bond cleavage is associated with production of free nucleic acid base.

The observations of Chang and Meares[132] that Co(III)·BLM and $h\nu$ in the absence of O_2 produce 3′-phosphoglycolate-modified ends accompanying strand scission and no malondialdehyde is quite unusual. These results contrast dramatically with those from Fe(II)·BLM and ionizing radiation damage studies,[136,137] where production of phosphoglycolate-modified ends requires O_2 to produce the presumed intermediates and ultimately base propenal. Interestingly, all sugar products produced via ionizing radiation damage (HO·) involving C–C bond scission have been shown to require the presence of O_2.[138,139] Therefore, the firm identification of 3′-phosphoglycolate-modified ends, the identification of the monomeric product accompanying its formation, and the mechanism of their production are important to unravel. Novel chemistry will most surely be identified.

VIII. Mn(II)·BLM

In addition to iron and cobalt, BLM is also capable of forming an active DNA-degrading complex with Mn(II) and Mn(III). However, the cofactors required for this activity are at present controversial.

The Hecht group[140] was the first to report studies with Mn(II)·BLM and found that its incubation with SV40 form I DNA resulted in strand scission, producing relaxed circular and linear duplex DNA. No scission was observed under anaerobic conditions, and no detectable malondialdehyde was produced. Mn(II)·BLM appeared to be about 10-fold less active than Fe(II)·BLM under identical experimental conditions.

In addition, the Hecht group also examined the chemistry of Mn(III)·BLM·B_2 in the presence of iodosobenzene by using the same approach as with Fe(III)·BLM activation. An analysis of the reaction of Mn(III)·BLM and C_6H_5IO with a number of olefins such as *cis*-stilbene afforded a profile of oxidized products similar to that obtained for Fe(III)·BLM or (tetraphenylporphinato)manganese(III) chloride and iodosobenzene. The Mn(III)·BLM system produced single- and double-stranded nicks in SV40 DNA; however, no data were shown on this point. In addition, no malondialdehyde was detected.

Shortly after the Hecht paper,[140] Burger et al.[141] reported that Mn(II)·BLM required H_2O_2 to degrade DNA, a clear contradiction of the Hecht findings. They found that malondialdehyde was formed and verified by TLC that thymine and thymine propenal were formed in a 5 to 1 ratio, a considerably higher ratio than that found for Fe·BLM (~1 to 1) in air. Mn(II)·BLM was determined to have 1–3% of the activity of Fe(III)·BLM with H_2O_2. Furthermore, they found that aerobic solutions of 2-mercaptoethanol were inactive, and the addition of thiols rapidly terminated the Mn^{II}·H_2O_2-mediated degradation.

Finally, Mn(II)·BLM was also investigated by Suzuki et al.,[142] who reported that the complex could cause DNA damage, as determined by sequencing gel analysis, in the presence of O_2 and a reductant (2-mercaptoethanol), or with H_2O_2 alone, or by irradiation with UV light. Their three induction systems afforded very similar nucleotide sequence cleavage patterns. In addition, the mobility of oligonucleotide fragments seems to suggest that 3′-phosphoglycolate ends were present to some extent, although this was not pursued.

It should be apparent from this discussion that major discrepancies exist in the literature on Mn(II)·BLM. Similar contradictory results are also apparent in the literature on Cu(I)·BLM (discussed below).[143,144] These discrepancies are probably indicative of metal contamination problems, and it is clear that to pursue meaningful experiments methods must be established to ensure that the metal of choice is responsible for the observed chemistry.

IX. Cu(I)/Cu(II)·BLMs

Cu(II)·BLMs and metal-free BLMs can inhibit the growth of tumor cells in tissue culture[145] and tumor growth in animals.[146,147] These results contrast dra-

SCHEME 12

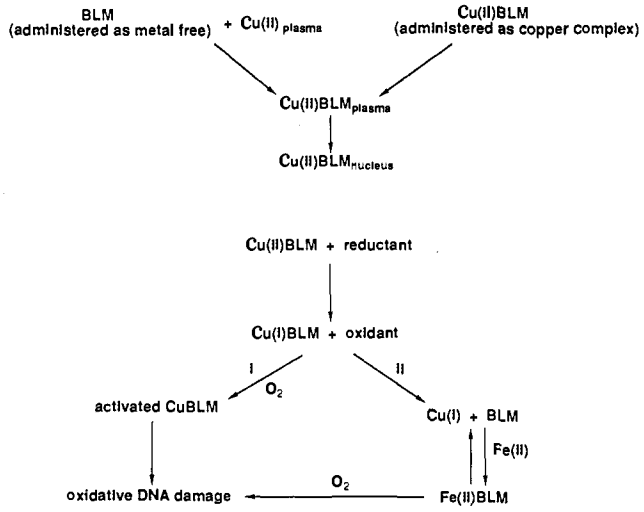

matically with in vitro studies with Cu(II)·BLM where numerous laboratories have shown its inability to degrade DNA, the molecular mechanism thought to be responsible for its cytotoxicity in vivo.[54,145,148] To account for this apparent inconsistency between the in vivo and in vitro data, two hypotheses were put forth (Scheme 12) by Umezawa and colleagues[148] and Hecht and colleagues.[143] Both models agree that free BLM rapidly forms Cu(II)·BLM in the plasma and that this is the species that is probably transported into the nucleus of the cell. Studies from Freedman et al.[149] and Antholine et al.[145] indicate that physiological reducing agents such as cysteine, glutathione, or perhaps thiols in proteins can reduce Cu(II)·BLM to Cu(I)·BLM, albeit at slow rates. Alternative physiological reductants such as NADPH-flavin and/or "FeS" proteins have also been considered, based on the 1-electron reduction potential of Cu(II)·BLM to Cu(I)·BLM of −329 mV.[150] Both Schuelen et al.[151] and Kilkuskie et al.[150] examined the possibility that NADPH-cyt P_{450} reductase, present in the nucleus or nuclear membrane, can mediate this reduction, which was monitored by measuring oxidative DNA damage. The results from these two laboratories are in disagreement. While this controversy still needs to be resolved, the chemical model studies[145,149] establish unambiguously that reduction occurs with thiols. At this point, the two models (Scheme 12) diverge. Hecht's model[143] considers Cu(I) a direct participant in the oxidative DNA damage and the Umezawa model[148] considers "Cu" as a prodrug, delivering BLM to the nucleus where it then becomes a spectator, and Fe(II) is responsible for oxidative DNA damage.

In support of the active role of Cu(I) in the oxidative damage, Hecht's laboratory[143] reported that Cu(II) or Cu(I) in the presence of dithiothreitol, dithionite, or the NADPH-dependent cyt P_{450} reductase is capable of converting supercoiled cccDNA, SV-40 or PM-2 DNA, to nicked circular and linear duplex DNA. They also reported that these reactions are O_2-dependent and that thymine, but no base propenal, is produced. In addition, Cu(II)·BLM in the presence of the O_2-surrogate iodosobenzene, and in the *absence* of external reductant, is also active in the supercoiled DNA nicking assay. These results, which strongly support Hecht's hypothesis, unfortunately are inconsistent with previous published data of a number of investigators.[145,152,153] Hecht and co-workers propose that the inconsistencies are related to differences in the copper concentrations employed [nicking was observed at concentrations of Cu(II) ≤ 25 μM]. However, a recent paper of Suzuki et al.[144] reported that, by using *φX174* DNA and conditions quite similar to those of Ehrenfeld et al.,[143] no cleavage by Cu(I)·BLM was detectable above background. Both laboratories did appropriate controls for artifacts resulting from low levels of contaminating Fe(III), which in the presence of DTT could mediate the oxidative DNA damage. Thus, the reason for these discrepancies is unclear and the ability of Cu(I)/Cu(II)·BLM to directly mediate DNA strand scission is still an important point that needs to be resolved. Light might be shed on this controversy if the specificity of Cu·BLM were examined by using standard [^{32}P]-end-labeled DNA fragments in place of the "highly" sensitive supercoiled DNA nicking assay. On the basis of the NMR studies of Cu(I)·BLM and the product analyses of Ehrenfeld et al.,[143] it is clear that the chemistry of the Cu system is different from the Fe system. These differences should be readily observed by using this technique.

Note Added in Proof. A recent paper by Ehrenberg et al.[196] has convincingly demonstrated the ability of Cu·BLM to degrade DNA in vitro.

The Umezawa model[148] (Scheme 12) requires that Cu(I)·BLM [K_a] ~ 4 times K_a of Fe(II)·BLM] combine with "Fe(II)" in the nucleus to produce Fe(II)·BLM, which is ultimately responsible for the oxidative DNA damage. While studies by both Freedman et al.[149] and Antholine et al.[145] indicate that this is a viable model in vitro, the extrapolation to in vivo conditions still warrants concern for the following reasons. First, the concentration of BLM and therefore Cu(II)·BLM in the nucleus is unknown but is quite low, and therefore Cu(II)·BLM should be entirely bound to the DNA. Second, the identity and concentration of the physiological reductant(s) are unknown [Recent studies from the laboratory of Peisach (Ciriola, M. R.; Magliozzo, R. S.; Peisach, J. *J. Biol. Chem.*, in press) provide evidence for the role of $O_2^{\cdot-}$ as the physiological reductant.], and reduction of a Cu(II)·BLM (already sterically hindered) bound to DNA would be even more difficult. Third, the concentration and source of Fe(II) in the nucleus is unknown. Future research will address these experimentally difficult questions, but at present the role of "Cu vs. Fe" BLMs as mediators of in vivo damage remains unanswered.

X. $(OP)_2Cu^I \cdot H_2O_2$-Mediated DNA Degradation

A. Proposed Chemistry

A recent excellent review by Sigman[3] provides an up-to-date summary of the substantial progress made by his laboratory in unraveling the chemistry of the oxidative nuclease activity of the $(OP)_2Cu^I$ and its cofactor H_2O_2.[154]

$(OP)_2Cu^I$ binds to double-stranded DNA and in the presence of H_2O_2 causes its rapid oxidative degradation. It preferentially degrades B-form DNA over A-form DNA and does not degrade Z-form DNA.[155,156] Thus, $(OP)_2Cu^I$ appears to recognize a helical conformation in the absence of any clear consensus sequence. The mechanism of binding, the role of the cofactors H_2O_2

and Cu(I), and the products resulting from oxidative destruction have been elucidated.[3,154-157]

B. Binding Mode

Studies on the interaction of $(OP)_2Cu^I$ with the Dickerson dodecamer 5′-CGCGAATTCGCG-3′ in the presence or absence of netropsin and the restriction enzyme *Eco*R1 provided strong support for the thesis that $(OP)_2Cu^I$ attacks DNA specifically from the minor groove without intercalation.[155] X-ray crystallographic studies of Kopka et al.[158] demonstrated that netropsin binds to the minor groove in the AATT region of the dodecamer. Observations that netropsin protects A-5, T-6, T-7, and C-9 from $(OP)_2Cu^I$ attack support the notion of minor groove chemistry. X-ray crystallographic studies of Rosenberg and his colleagues[159] demonstrated that a tridecamer containing the dodecamer in the absence of Mg(II) binds to *Eco*R1 specifically by major groove interactions. The minor groove in this complex is accessible to solvent. In addition, the hydrogen-bonding network between the tridecamer and *Eco*R1 would preclude any intercalative interactions of $(OP)_2Cu^I$ with DNA. As predicted by this model, *Eco*R1 does not protect the dodecamer from oxidative attack.

C. Specificity of Nuclease Activity

2,9-Substituted derivatives of *ortho*-phenanthroline (OP) are ineffective nucleases, presumably due to inappropriate complex formation with copper. 4,7-Substituted OPs are inactive when phenyl is the substituent. Molecular modeling implies that the steric bulk of the phenyl(s) precludes binding in the minor groove. A variety of substitutions have been shown to be tolerated at the 5-position, although the rates of nuclease cleavage are altered.[3]

D. Role of Cu(I) and H_2O_2

Early studies indicated that catalase inhibited oxidative damage, and $O_2^{\cdot-}$ in the presence of $(OP)_2Cu^{II}$ stimulated oxidative damage. These observations recently were accommodated in eq 9, proposed by Graham et al.[157] The superoxide can reduce Cu(II) to Cu(I)

$$(OP)_2Cu^{II} + O_2^{\cdot-} \rightarrow (OP)_2Cu^{I} + O_2 \quad (9a)$$

$$2O_2^{\cdot-} + 2H^+ \rightleftarrows H_2O_2 + O_2 \quad (9b)$$

$$(OP)_2Cu^{I} + H_2O_2 \rightarrow (OP)_2Cu^{II} + HO\cdot + HO^- \text{ or } (OP)_2[CuOH]^{2+} \quad (9c)$$

(eq 9a) and also undergo a dismutation reaction to generate H_2O_2 (eq 9b). Thus, both cofactors are produced, which can then undergo Fenton-type chemistry[160] responsible for the oxidative damage (eq 9c). The observed product distribution of this damage, discussed subsequently, argues in favor of metal-ion-complexed active species $[CuO]^{1+}$ rather than a freely diffusable HO· radical.

E. Product Production

The most insightful product analysis of $(OP)_2Cu^I$·H_2O_2-mediated DNA damage was obtained by using 3′- and 5′-[^{32}P]-end-labeled DNA fragments and gel electrophoresis. These methods allowed Sigman and colleagues to conclude that strand scission is accompanied by the production of large amounts of 3′- and 5′-phosphomonoester termini, much smaller and variable amounts of 3′-phosphoglycolate termini and, quite intriguingly, a metastable 3′-intermediate whose stability may be sequence specific.

SCHEME 13

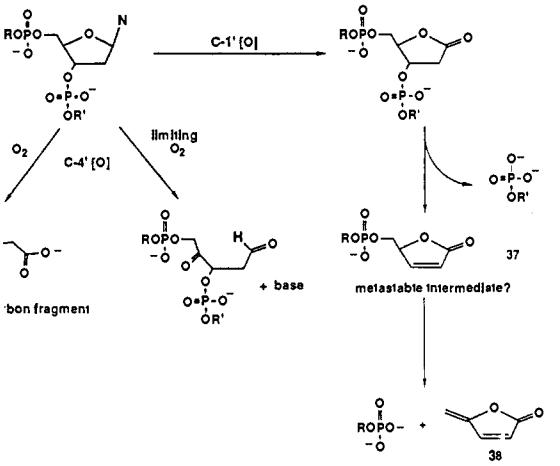

An important distinction between the $(OP)_2Cu^I$ and Fe·BLM systems is that in the former case the 3′-phosphate termini and strand scission are produced under normal physiological conditions, while in the latter case their production requires alkali [OH^-] conditions. This difference is consistent with the differences in the proposed chemistry outlined below.

The monomeric products produced by $(OP)_2Cu^I$-mediated oxidative damage have thus far been identified as free nucleic acid bases. No base propenals have been detected, although appropriate controls indicate stability of authentic base propenals to the isolation conditions.[195] These results contrast with Fe·BLM chemistry, where equal amounts of base propenal accompany phosphoglycolate termini production.[15,16] In addition, these results contrast with those of methidium-propyl-EDTA·Fe[161] and pulse radiolysis studies,[136,162] both "HO·" generators, where approximately equal amounts of 3′-phosphate termini and 3′-phosphoglycolate termini are observed.

Perhaps the best argument in support of minor groove attack is that the observed products can be attributed to chemistry at C1′ and C4′ of the deoxyriboses, the two hydrogens in B-form DNA most accessible from the minor groove. The hypothesis to account for present experimental facts is outlined in Scheme 13. Sigman[3] and Uesugi et al.[163] proposed that the primary mode of attack is hydrogen atom abstraction from the 1′-carbon by HO· or an active $[CuO]^+$ or $[CuOH]^{2+}$ species. Since the 1′-hydrogen is less accessible in the minor groove than the 4′-hydrogen, this result suggests that the metal is playing a directive role. They propose that oxidation occurs at the 1′-carbon to produce a deoxyribonolactone site concomitant with loss of free nucleic acid base. The 2′-hydrogens are proposed to be acidic enough so that under physiological conditions intermediate **37** and 5′-phosphate ends (strand scission) are produced. This "metastable intermediate" **37** was shown to undergo a presumed second elimination under basic conditions to yield **38** (Scheme 13) and 3′-phosphate termini. This model predicts that **38** should be a monomeric product of this

reaction, and it has in fact been recently isolated and identified (GC–MS) by Sigman's laboratory.[195] Additional support for this proposal comes from studies of Uesugi et al.,[163] who showed that d(CG) in the presence of $(OP)_2Cu^I$ resulted in the production of cytosine (2%), guanine (2.1%), 5′-dGMP (2.1%), a (1.6%), and b (2.4%). Compound b is the expected product produced

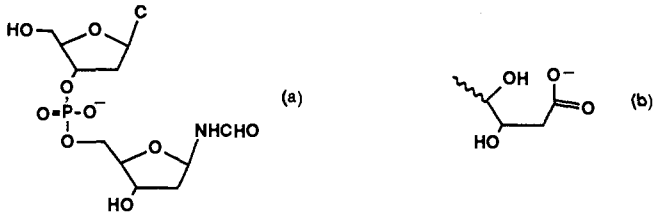

by 1′-C–H bond cleavage, while a is a product resulting from HO· and O_2 attack on the base moiety. Base destruction mediated by HO· generated by pulse radiolysis methods accounts for ~80% of the observed chemistry. Hence, it is perhaps not surprising that such a product has been identified in the $(OP)_2Cu^I$ system.

The minor pathway resulting in production of the presumed 3′-phosphoglycolate termini is more speculative and is proposed to proceed by chemistry initiated at the C4′ position. The chemistry resulting in production of "3-phosphoglycolates" and no base propenals is an enigma. The glycolate ends should be isolated and unambiguously identified. In addition, it would be of interest to know if their production is O_2 dependent. In the absence of O_2, hydroxylation at C4′ resulting in base production and alkali-labile strand production might be expected. Finally, given the conformational specificity of $(OP)_2Cu^I$, it would be of interest to make specifically 1′- and 4′-[^{2}H]DNAs and examine the resulting product distribution and its relationship to DNA conformation.

XI. Methidium-Propyl-EDTA (MPE)·Fe

Elegant studies from the Dervan laboratory[161,164,165] reported the tethering of a metal chelator arm, EDTA, to a DNA intercalator, methidium. Methidium-propyl-EDTA (MPE) and other members of this class in the presence of Fe(II), O_2, and reductant or Fe(III) and H_2O_2 are artificial nucleases capable of nonspecifically degrading DNA (RNA). These compounds have gained rapid recognition as footprinting agents, useful in defining the location of small ligands that bind to DNA. These synthetic nucleases, due to their small size and lack of specificity, have allowed a more accurate resolution of binding sites' sizes than DNase. A recent excellent review by Dervan[4] focuses on their efforts and successes in extending these studies to make sequence-specific DNA binding molecules attached to cleavers, to ultimately make artificial restriction enzymes. This section will focus, however, on the "DNA-cleaving" part of reagent Fe·EDTA, the proposed chemistry to account for observed oxidative damage, and the relationship of this chemistry to Fe·BLMs.

A. Binding Mode

Methidium, structurally similar to the classic intercalator ethidium, was originally attached to an EDTA arm in an effort to produce a compound that could act as an intercalative DNA binder delivering oxidizing equivalents to the DNA target. Studies by Hertzberg and Dervan[161] showed that MPE·Mg(II) and MPE·Ni(II) [MPE·Fe(II) binding cannot be measured because of rapid DNA destruction] have binding affinities for calf thymus DNA of 1.5×10^5 M^{-1} and 1.2×10^5 M^{-1}, respectively. As a control, the ethidium binding constant was found to be 8×10^5 M^{-1} under similar conditions. The unwinding angle, an indicator of a molecule's intercalative abilities, was calculated to be 11 ± 3°/bound molecule of MPE·Mg(II) with supercoiled PM-2 DNA. This value compares with one of 26° determined for ethidium. Further studies are required to establish the hypothesis that MPE binds to DNA by an intercalative mode. The binding of the Fe·EDTA arm to the major, minor, or both groove(s) has not yet been established, although the observed chemistry suggests a minor groove interaction.

B. Chemistry of Cofactors Fe(II), O_2, Reductant, and Fe(III)·H_2O_2

Studies of Hertzberg and Dervan[161,164] showed that Fe(II)·O_2·MPE and reductant cleaves DNA several orders of magnitude more rapidly than EDTA-Fe(II) under identical conditions. In addition, they also showed that catalase and SOD, superoxidase dismutase, as well as high concentrations of reductant DTT, a known radical scavenger, inhibit this oxidative damage. MPE·Fe(III)·H_2O_2 can replace Fe(II), O_2, and reductant to give similar, but not identical, product distributions. Moreover, EDTA·Fe(II), at concentrations several orders of magnitude higher than used with MPE·Fe(II), also produces similar products.

Recent efforts have been directed toward developing model systems to aid in understanding the chemistry affiliated with nonheme iron biological systems. The interactions of Fe(II) and H_2O_2 (Fenton's reagent),[160] Fe(II), EDTA, and H_2O_2,[166] as well as those of EDTA·Fe(III) with H_2O_2 and peracids,[167] have been examined in some detail and are directly pertinent to chemistry responsible for oxidative damage in the Fe·MPE system.

The oxidation of a substrate, R_xH, with Fenton's reagent has been proposed to involve the steps outlined in Scheme 14 with measured rate constants k in M^{-1} s^{-1}.

SCHEME 14

(1) $H_2O_2 + Fe^{++} \xrightarrow{k_1} Fe^{3+} + HO\cdot + HO^-$ $k = 76$

(2) $HO\cdot + Fe^{2+} \xrightarrow{k_2} HO^- + Fe^{3+}$ $k = 3 \times 10^6$

(3) $HO\cdot + R_aH \xrightarrow{k_{3a}} R_a\cdot + H_2O$

$HO\cdot + R_bH \xrightarrow{k_{3b}} R_b\cdot + H_2O$ $k = 10^7$–10^{10}

$HO\cdot + R_cH \xrightarrow{k_{3c}} R_c\cdot + H_2O$

(4) $R_a\cdot + Fe^{3+} \xrightarrow{k_4} R_a^+ + Fe^{2+}$

(5) $2R_b\cdot \xrightarrow{k_5} R_b\text{–}R_b$

(6) $R_c\cdot + Fe^{2+} \xrightarrow{k_6} R_c^- + Fe^{3+}$

$R_a\cdot$, $R_b\cdot$, and $R_c\cdot$ are three different types of radicals produced that, depending upon their structure, undergo oxidation (Scheme 14, 4), dimerization (Scheme 14, 5),

or reduction (Scheme 14, 6).[160]

Data obtained with a variety of "substrates" allowed a dissection of relative rates of attack on different C–H bonds. A comparison with similar rates of attack determined from radiation chemistry (using pulse radiolysis and competition experiments), where the active species is known to be HO·, within the large errors of the method, allowed validation of the proposed scheme.

However, the nature of the active oxidant is still controversial (eq 10) and, in contrast to the hydroxyl radical proposed in Scheme 14, has also been proposed to be an "iron–oxo" species.[166,168,169] These ferryl species

$$H_2O_2 + Fe(II) \rightleftarrows [Fe^{II}OH]^{3+} + H_2O \rightleftarrows [Fe^{II}O]^{2+} \quad (10)$$

are kinetically equivalent to HO· in all reactions shown in Scheme 14. At present, therefore, one can only say that a "HO·" equivalent is responsible for the oxidative damage.

Dervan's MPE·Fe(II)-inflicted damage is dependent on O_2 and a reductant. Presumably, the Fe(II) is rapidly oxidized by O_2 to Fe(III) and $O_2^{\cdot-}$. The latter in protic media rapidly disproportionates to produce H_2O_2. The Fe(II) and H_2O_2 present can then, as indicated in Scheme 14, catalyze production of the active oxidant. If the oxidant is indeed freely diffusable HO·, damage to both bases and to the deoxyribose moiety of the nucleotide backbone of DNA might be expected. The actual products produced will be discussed subsequently.

In addition, Fe(III)·MPE·H_2O_2 was also examined for DNA cleaving ability by Dervan and co-workers.[161] The chemical mechanism of Fe(III)·EDTA-catalyzed decomposition of H_2O_2 was studied by Walling and coworkers,[170,171] and shown to be a complex function of both pH and concentrations of species used. Walling studied the kinetics of retardation of H_2O_2 decomposition by substrates such as acetone and *tert*-butyl alcohol, which can be oxidized by this system. These studies led him to conclude that degradation of H_2O_2 involves a HO· chain pathway (Scheme 15), the relative contribution of each step being dependent on the reaction conditions.

SCHEME 15

$$Fe(III) + H_2O_2 \rightarrow Fe(II) + H^+ + HO_2\cdot$$

$$Fe(II) + H_2O_2 \rightarrow Fe(III) + HO\cdot + HO^-$$

$$HO\cdot + H_2O_2 \rightarrow H_2O + HO_2\cdot$$

$$HO_2\cdot + Fe(III) \rightarrow Fe(II) + H^+ + O_2$$

$$HO_2\cdot + Fe(II) \rightarrow HO_2^- + Fe(III)$$

$$HO\cdot + RH \rightarrow R\cdot + H_2O$$

$$R\cdot + O_2 \rightarrow RO_2\cdot \xrightarrow{Fe(II)} ROOH + Fe(III)$$

As indicated in the previous sections, the chemistry involved in production of the active oxidant and its subsequent reactions is quite complex. If freely diffusible HO· is indeed the oxidant, then the products produced might be expected to be many and more varied than those observed with the Fe·BLM system.

C. Products of DNA Degradation

Incubation of MPE·Fe(II), O_2, and reductant with 3′- and 5′-[^{32}P]-end-labeled DNA restriction fragments and subsequent analysis using high-resolution denaturing gel electrophoresis gave the first clues regarding product production. Hertzberg and Dervan[161] reported that under these conditions 5′-phosphate termini and equivalent amounts of 3′-phosphate and 3′-phosphoglycolate termini were observed. The 3′-phosphoglycolate termini were unambiguously identified by chemical and enzymatic degradation of the damaged DNA, followed by GC–MS analysis of the derivatized glycolic acid. Production of 3′-phosphate termini occurred under assay conditions (neutral pH) in analogy with their production by ^{59}Co pulse radiolysis[162,172,173] and by $(OP)_2Cu^I \cdot H_2O_2$,[3] and in contrast with their production by BLM where alkali treatment is required.

Furthermore, if MPE·Fe(III) and H_2O_2 replace MPE·Fe(II), O_2, and reductant to effect strand scission, the products thus far examined are similar, except that the amount of 3′-phosphate termini appeared to increase at the expense of 3′-phosphoglycolate termini. This ratio of 3′-phosphate termini to 3′-phosphoglycolate termini is similar to that observed in the $(OP)_2Cu^I$ system and differs from the ~1:1 ratio observed in the Fe(II), O_2, and pulse radiolysis protocols.

Monomeric products were also isolated and identified by Hertzberg and Dervan to be all of the possible nucleic acid bases. The relative amounts of the bases produced is directly related to their statistical distribution in DNA, and one base is released per cleavage event. Efforts to detect base propenals equivalent to the amount of phosphoglycolate termini were unsuccessful. These results are analogous to those observed with $(OP)_2Cu^I$[3] and contrast with those from pulse radiolysis studies.[136] The monomeric species produced accompanying 3′,4′ C–C bond cleavage thus remains to be elucidated.

D. Proposed Mechanism

All of the above considerations led Hertzberg and Dervan[161] to propose that MPE·Fe(II) in the presence of O_2 and reductant generates HO· near deoxyribose residues in the minor groove of DNA. In analogy with the $(OP)_2Cu^I$ chemistry proposed by Sigman and coworkers (Scheme 13),[3] hydrogen atom abstraction could occur at either the C1′ or C4′ positions of the deoxyribose ring. Hydrogen atom abstraction from the 1′-position could produce a 1′-carbon radical. This intermediate could be effectively oxidized by MPE·Fe(III), as would be the case with $(OP)_2Cu^{II}$. [In general, copper is a much less discriminating radical oxidant than Fe(III).[160]] Addition of H_2O to the carbonium ion would produce the hemiaminal, which would collapse to release base and a deoxyribonolactone-containing oligomer. [This carbonium can be stabilized by either the unpaired electrons of O or N attached to C1, and hence is readily produced by Fe(III) reduction. Interestingly, Fe(III) probably mediates carbonium ion production by an outer-sphere e^- transfer. On the other hand, Cu(II) oxidations, which are significantly slower than the fastest ones observed with Fe(III), and whose ligand exchange rates are rapid, can mediate carbonium ion production through an intermediate organo-copper species.]

As in the case of $(OP)_2Cu^I$, the chemistry at the 4′-position is more obscure. The requirement for O_2, the mechanism by which the 3′-phosphoglycolate termini

SCHEME 16

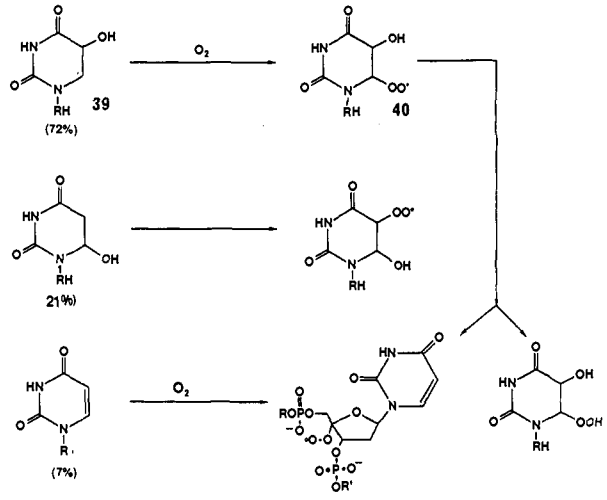

are produced, and the nature of the 3-carbon fragment accompanying termini production are of interest to establish.

An alternative mode(s) to the direct HO·-mediated hydrogen atom removal from deoxyribose, based on recent pulse radiolysis studies examining HO·-mediated DNA degradation,[139,173,174] needs to be considered (Scheme 16). In pulse radiolysis experiments, hydroxide radical reacts much more prevalently with bases such as thymine to produce 5-hydroxy-6-radical species **39** than with deoxyribose moieties. This radical base species **39** rapidly reacts with oxygen to produce a 6-peroxy radical **40**, which is proposed to be responsible for hydrogen atom abstraction from a deoxyribose moiety not attached to the modified base. This alternative model predicts that base destruction would accompany strand scission events and also needs to be considered in the MPE·Fe(II) system.

In contrast with the chemistry outlined above occurring in the minor groove, an alternative mechanism, which presently cannot be ruled out, involves chemistry of MPE·Fe(II) occurring in the major groove. Scheme 17 accounts for base release and production of the 3′- and 5′-phosphate termini. The 3′-hydrogen of the deoxyribose moieties in the major groove is most accessible to abstraction, and HO·-mediated hydrogen atom abstraction would produce the 3′-deoxyribosyl radical. Oxidation of this radical by Fe(III)·EDTA and addition of H_2O to the carbonium ion at the 3′-position would produce a 5′-phospho-3′-keto-deoxynucleotide **41** and 5′-phosphate termini under physiological conditions. [Oxidation by Fe(III) is selective and parallels stabilities of the corresponding carbonium ions. The proposed secondary carbonium (Scheme 17) is not very stable and hence makes this pathway less likely.] This species **41** could rapidly lose both base and 5′-phospho oligomer to generate the monomeric product 2-methylene-3-(2*H*)-furanone **42**. This compound has previously been characterized as the species responsible for inactivation of ribonucleotide reductases when these enzymes are incubated with 2′-chloro-2′-deoxynucleotides (eq 7).[121] This monomeric product is readily trapped by ethanethiol to produce

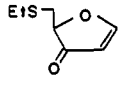

The proposed mechanism of base release (outlined in

SCHEME 17

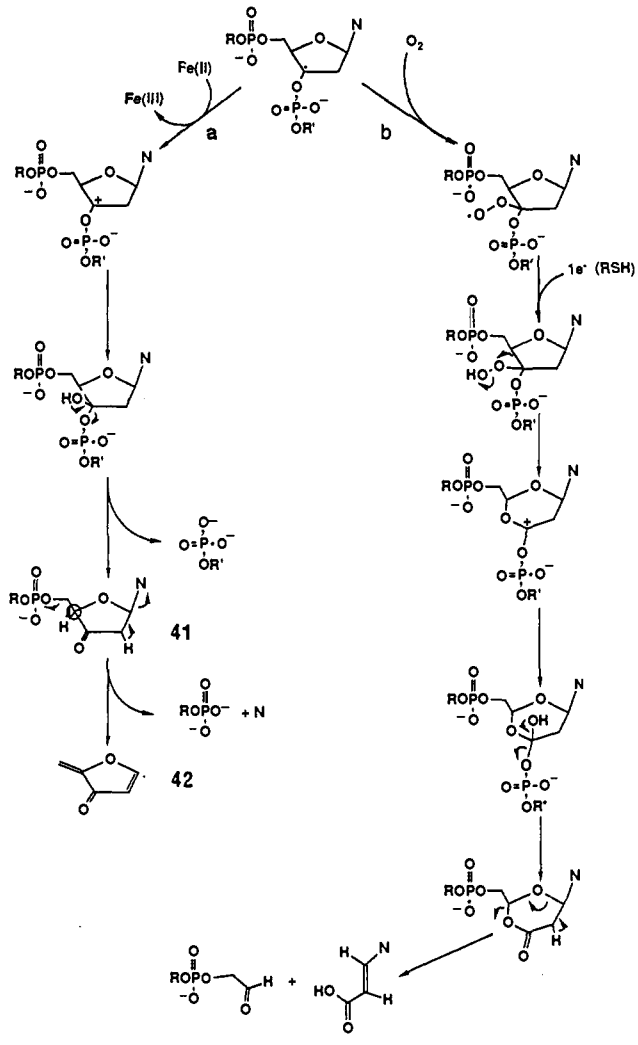

Scheme 17a is readily testable by using 3′-[^{3}H]DNA models to establish 3′-carbon–hydrogen bond cleavage and 5′-[^{3}H]DNA models in the presence of an EtSH trap to establish formation of 2-methylene-3(2*H*)-furanone.

If the chemistry of MPE·Fe is occurring from the major groove, then the production of 3′-phosphoglycolate termini and no base propenals must also be explained. A proposal outlined in Scheme 17b and described subsequently is not entirely satisfactory. However, neither has a satisfactory proposal been made involving minor groove chemistry. In order to obtain 3′,4′ carbon–carbon bond scission, O_2 addition to the 3′-radical would be required to form the 3′-peroxy radical intermediate. This peroxy radical would then be reduced to form the 3′-Fe peroxide complex, which could undergo a Criegee-type rearrangement (facilitated by the Lewis acid nature of the iron) to produce 3′-phosphoglycolaldehyde termini and base propenoate. [Thiols (pH 6.1–7.6) can reduce such species with rate constants of 0.8–1.3 × 10^5 dm^3 mol^{-1} s^{-1}. At higher pH the thiolates can mediate reduction via rapid e$^-$ transfer.[174]] This latter compound could be rapidly hydrolyzed to give strand scission and 5′-phosphate termini along with base propenoic acids, which would not be expected to react with thiobarbituric acid. The 3′-phosphoglycolaldehyde would have to be oxidized to glycolic acid, isolated, and identified by Hertzberg and Dervan[161] under the conditions employed to account for

their reported results. A distinction between the minor groove and major groove alternative pathways is possible with specifically [^{3}H]labeled DNA models.

XII. Ionizing Radiation Damage

Damage of DNA by ionizing radiation occurs in vitro and in vivo, and in the latter case exerts cytotoxic, mutagenic, and carcinogenic effects on exposed cells. Both single-stranded and double-stranded DNA scission have been shown to occur, uniformly and independent of DNA sequence.[175] Numerous lesions, responsible for strand scission, occur in very low yields, and as a consequence it has not been easy to elucidate the mechanisms responsible for the observed lesions. Identification of lesions can be accomplished by two complementary methods. The first involves isolation and identification of the small molecules produced.[108,138] The second involves determination of the end groups resulting from strand scission.[162,175] Furthermore, because of the multiple products produced, the γ-radiolysis products have been further subdivided into those resulting from anoxic and those from aerobic conditions.

Identification of the modified sugar residues isolated and intensive investigation of the chemistry of simpler polyhydroxy model compounds allow speculation concerning the mechanism(s) [$\pm O_2$] by which the products are produced. Ultimately, design of experiments to distinguish between various proposals can be initiated. The reader is referred to several excellent reviews in this area.[108,138] Only the salient features relevant to BLM will be summarized.

A. Identification of Modified Sugar Fragments

While the vast majority of damage inflicted by γ-radiolysis is on the "base" moiety of nucleotides of DNA, discussion here will be restricted to damage of the deoxyribose component either directly by HO· or indirectly by base–peroxy radical mediated hydrogen atom abstractions.[139,176] Methods, both chemical and enzymological, have been developed to analyze the modified sugars released directly during γ-radiolysis or released subsequent to γ-radiolysis and chemical treatment.[177] The products thus far isolated and identified by GC–MS, subsequent to $NaBD_4$ reduction and derivatization, are shown in Figure 9. The distribution of products is dependent on temperature, pH, concentration, and the presence or absence of O_2. It is clear that chemistry can happen at every position on the sugar moiety. While the chemistry at C3′ has not been included in Figure 9, recent results have also postulated chemistry occurring at C3.[139] We will focus on a specific subset of this tremendously complicated set of reactions: chemistry happening at the C4′ position and its relationship to that postulated for BLM.

B. Anaerobic γ-Radiolysis: Chemistry at C4′

In analogy with BLM, HO·-mediated hydrogen atom abstraction (Scheme 18) results in "free base release" and production of a variety of 4′-ketone sugar moieties **17–20** (Figure 9). However, in contrast with BLM, base release is accompanied by "immediate" strand scission; whereas with BLM, strand scission occurs only subsequent to treatment with alkali. Thus, the mechanism(s)

SCHEME 18. Mechanism of Base Release under Aoxic Conditions Mediated by C4′ Radical Chemistry[108]

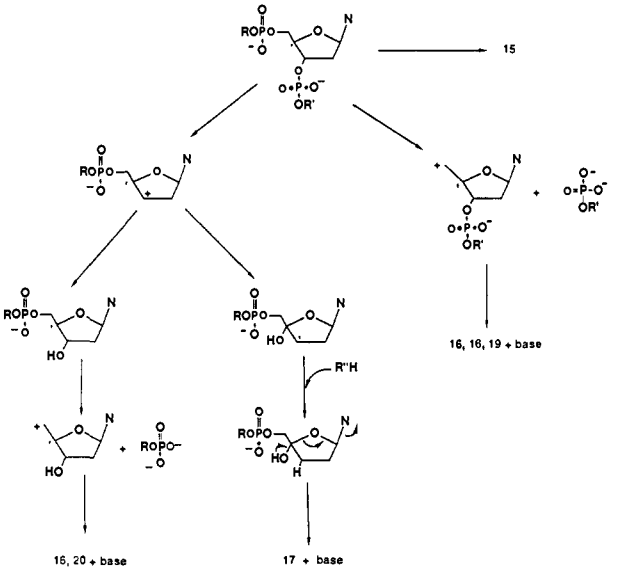

proposed in Scheme 18 to account for product production mediated by γ-radiolysis are not adequate to account for BLM chemistry.

The basic theme of Scheme 18 involves cation radical intermediates and is based on extensive rapid-flow EPR model studies using 2-methoxyethylphosphoric acids ($CH_3OCH_2CH_2OPO_3H_2$).[178,179] The rate constants for elimination of phosphate were measured by EPR and product production as a function of pH using ^{60} γ-radiolysis. The rate of elimination for the fully protonated derivative (PO_3H_2) is 3×10^6 s^{-1} and for the monoprotonated species is $CH_3OCH_2CH_2OPO_3H^-$ $\sim 10^3$ s^{-1}. This elimination, in the absence of any radical scavengers such as thiols or metals,[180] results in immediate strand scission. The resulting products are produced by addition of H_2O to the cation and chain termination by hydrogen atom abstraction from some RH in solution.

C. Aerobic γ-Radiolysis: Chemistry at C4′

In the case of aerobic γ-radiolysis of DNA, the chemistry at C4′ is probably much more complex than that observed with BLM even though several of the products produced are identical with those characterized for the BLM-mediated DNA degradation (Scheme 16).

Hydrogen atom abstraction from C4′ can be mediated directly by HO· or, as recently suggested from studies using poly(dU), by HO· addition to base moiety to produce the 5-OH-6-yl radical, which rapidly adds O_2. The base peroxy radical is postulated to be responsible for H atom abstraction from a different deoxyribose moiety.[139] How frequently this latter pathway is involved in hydrogen atom abstraction during γ-radiolysis of DNA remains to be established. However, due to the constraints of the double helical DNA structure, it would clearly not be as predominant as in the single-stranded poly(dU) case studied.

Under aerobic conditions O_2 can be added to the C4′ radical in a diffusion-controlled fashion ($k = 10^9$ M^{-1} s^{-1}). At concentrations of O_2 of 0.1 mM, this reaction should compete favorably with elimination of phosphate to form cation radical intermediates (Scheme 18). DNA

peroxy radicals (structures undefined) are observable with time-resolved EPR methods due to their characteristic g values = 2.01 and their unusually long lifetime when bound to nucleic acids (0.2–3.3 s). The lifetime of the peroxy radicals and their rate constants for reactions with thiols have been measured.[107] As discussed above, in the case of poly(dU), the base peroxy radicals were reported to be the major mediator of hydrogen atom abstraction of the deoxyribose ring.[139,176] In analogy with BLM a 4′-peroxy radical is proposed to be generated and to be an intermediate on the way to product production.

Recent studies from the laboratory of Haseltine and co-workers[136,162,175] identified at least two of the products presumably resulting from 4′-C–H bond cleavage. They studied ^{60}Co γ-irradiation effects on 3′- and 5′-[^{32}P]-end-labeled DNA fragments, using high-resolution gel electrophoresis to analyze the damage.[162,175] The results show that under aerobic conditions 5′-phosphorylated ends and equivalent amounts (the ratio varies from 0.7 to 1.1) of two distinct 3′-phosphorylated ends are produced. Chemical and enzymatic analyses established that the 3′-ends that migrate more slowly electrophoretically are phosphorylated and the more rapidly migrating 3′-ends contain a 3′-phosphoglycolate moiety. These are the same types of ends observed in BLM-mediated DNA degradation; however, the 3′-phosphate ends with BLM are only observed subsequent to alkali treatment in contrast with their production under neutral conditions with γ-irradiation.

These studies were recently extended by Janieck et al.[136] to identify the sugar moiety(ies) that may accompany phosphoglycolate production. Careful analysis of model compounds (3′, 5′-TDP, 3′-TMP, 5′-TMP, thymidine) and DNA allowed them to identify base propenals. These results account, at least in part, for the previous reports of malondialdehyde production, using the thiobarbiturate (TBA) assay, by other workers in the field.[108,138] However, no direct correlation between thymine propenal and phosphoglycolate production has been reported. In DNA, the production of thiobarbituric acid positive material requires O_2. However, irradiation of thymidine gave a positive thiobarbituric acid test in the *absence* of O_2, by a mechanism that remains to be elucidated.

In addition, and in analogy with recent reports of Burger et al.,[120] 80% of the TBA-reactive material is initially EtOH precipitable, indicating that the precursor to base propenal is still part of a DNA strand. The rate at which this precursor is converted to base propenal would be of interest to compare with recent efforts of Burger et al.[120] to establish a similar precursor–product relationship with BLM damage, where the $t_{1/2}$ = 40 min at 0 °C. Finally, unpublished studies of Schulte-Frohlinde and Bothe[173] indicate that the amount of glycolate equals the amount of malondialdehyde. The laboratories of von Sonntag and Schulte-Frohlinde proposed a chemical model (Scheme 19) to account for their results,[108,138] which is substantially different from that proposed by Janieck et al., which is analogous to the BLM model (Scheme 20).

The mechanism proposed in Scheme 19 is based on extensive studies on small molecule peroxy radicals and poly(U) peroxy radicals,[103,108] in which two peroxide radicals are proposed to dimerize to form tetraoxides.

SCHEME 19

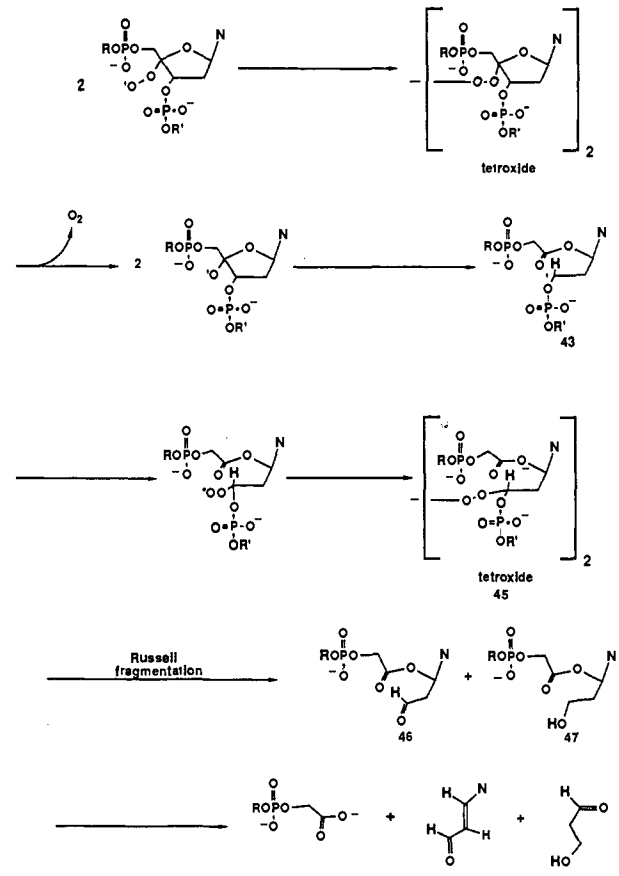

SCHEME 20

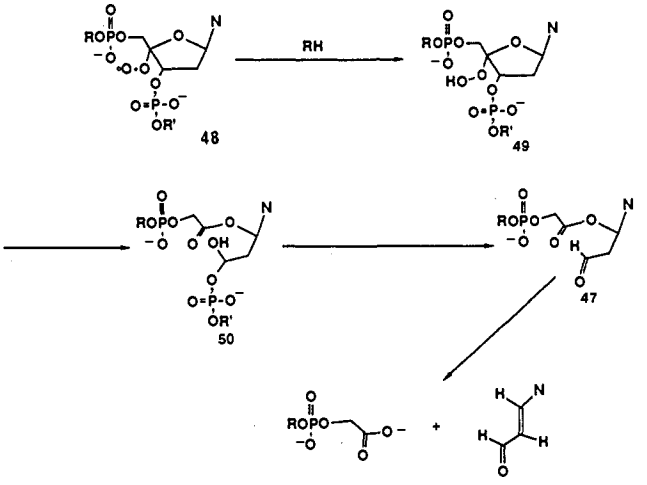

Ingold reported that tertiary tetraoxides, in contrast with the primary and secondary ones, slowly collapse to liberate O_2 gas and the tertiary oxy radicals. This type of radical species can rapidly undergo carbon–carbon bond scission to generate a 3′-carbon radical **43** (Scheme 19). Compound **43** can then rapidly (diffusion control) react with an additional molecule of O_2 to form the new peroxy radical **44**, which can dimerize to form **45**, a new tetraoxide (dimerization could occur with any peroxide radical, i.e., self-condensation is not required). Compound **45** has a hydrogen α to the tetraoxide, which would allow it to undergo a concerted Russel fragmentation to produce **46** and **47** and O_2. Compound **46** is the direct precursor to base propenal and the phosphoglycolate-modified end and is identical with that proposed by Janieck et al. (Scheme 20). The proposal

SCHEME 21

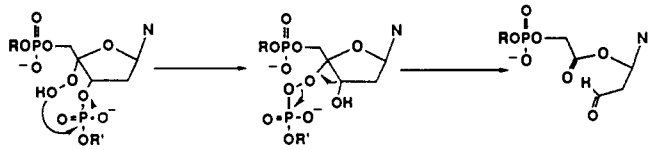

as outlined in Scheme 19 has ample precedent in small molecule model systems. However, whether similar tetraoxides can be generated with DNA substrates, conformationally and sterically restricted due to the defined structure, is a question requiring further experimentation.

The mechanism proposed by Janieck et al.,[136] which requires much fewer transformations and is based on analogy with BLM, at first seems quite appealing. However, conversion of the 4′-hydroperoxide **49** to **50** via a "Criegee"-type rearrangement is problematic. In model systems[110] this rearrangement requires strong acid catalysis or acylation.[117] In the case of BLM it has been proposed that metal center can catalyze this reaction, although this has not yet been substantiated. Therefore, for the Janieck et al.[136] mechanism to be chemically reasonable would require perhaps acylation of the terminal oxygen of the peroxide by the 3′-phosphate of DNA (Scheme 21). This would facilitate heterolytic cleavage of the O–O bond, allowing a Criegee-type rearrangement, and ultimately production of **47** (Scheme 20). Studies from our laboratory[105] using [3′-^{18}O]poly(dAdT) showed that similar chemistry does not occur with BLM, as this mechanism requires P–O rather than the observed C–O bond cleavage.

Given the complexity of the products produced on γ-irradiation of DNA, recent elegant studies from a number of laboratories[108,138,162,175] are beginning to unravel these intriguing mechanisms as evidenced by studies described above for the C4′ radical.

Acknowledgments. We acknowledge our co-workers without whom our small contribution to understanding the mechanism of BLM-mediated degradation would not have been possible: John Wu, Lois Rabow, Glen McGall, Sudhir Adjmera, and Leroy Worth.

Registry No. BLM, 11056-06-7.

XIII. References

(1) Umezawa, H. In *Bleomycin: Chemical, Biochemical, and Biological Aspects*; Hecht, S. M., Ed.; Springer-Verlag: New York, 1979; p 24, footnote
(2) Goldberg, I. H.; Kappen, L. S.; Chen, D. H. In *Cellular Regulation and Malignant Growth*; Ebashi, S., Ed.; Japan Society: Tokyo, Springer-Verlag: Berlin, 1985; p 483.
(3) Sigman, D. S. *Acc. Chem. Res.* **1986**, *19*, 180.
(4) Dervan, P. B. *Science (Washington, D. C.)* **1986**, *232*, 464.
(5) Barton, J. K. *Science (Washington, D.C.)* **1986**, *233*, 727.
(6) Umezawa, H.; Maeda, K.; Takeuchi, T.; Okami, Y. *J. Antibiot., Ser. A* **1966**, *19*, 200.
(7) Umezawa, H. In *Bleomycin: Current Status and New Developments*; Curter, S. K., Crooke, S. T., Umezawa, H., Eds.; Academic: New York, 1978; p 15, footnote.
(8) Umezawa, H. *Lloydia* **1977**, *40*, 67.
(9) Umezawa, H. *Pure Appl. Chem.* **1971**, *28*, 665.
(10) Umezawa, H. *Biomedicine* **1973**, *18*, 459.
(11) Hecht, S. M. *Acc. Chem. Res.* **1986**, *19*, 83.
(12) Takeshita, M.; Grollman, A. P.; Ohtsubo, E.; Ohtsubo, H. *Proc. Natl. Acad. Sci. U.S.A.* **1978**, *75*, 7983.
(13) D'Andrea, A. D.; Haseltine, W. A. *Proc. Natl. Acad. Sci. U.S.A.* **1978**, *75*, 3608.
(14) Burger, R. M.; Peisach, J.; Horwitz, S. B. *J. Biol. Chem.* **1981**, *256*, 11636.
(15) Giloni, L.; Takeshita, M.; Johnson, F.; Iden, C.; Grollman, A. P. *J. Biol. Chem.* **1981**, *256*, 8608.
(16) Burger, R. M.; Berkowitz, A. R.; Peisach, J.; Horwitz, S. B. *J. Biol. Chem.* **1980**, *255*, 11832.
(17) Takita, T.; Umezawa, Y.; Saito, S.; Morishima, H.; Naganawa, H.; Umezawa, H.; Tsuchiya, T.; Miyake, T.; Kageyama, S.; Umezawa, S.; Muraoka, Y.; Suzuki, M.; Otsuka, M.; Norita, M.; Kobayashi, S.; Ohno, M. *Tetrahedron Lett.* **1982**, *23*, 521, 529.
(18) Aoyagi, Y.; Suguna, H.; Katano, K.; Primeau, J.; Chang, L. H.; Hecht, S. M. *J. Am. Chem. Soc.* **1982**, *104*, 5537.
(19) Kross, J.; Henner, D.; Haseltine, W. A.; Rodriguez, L.; Levin, M. D.; Hecht, S. M. *Biochemistry* **1982**, *21*, 3711.
(20) Fisher, L. M.; Kuroda, R.; Sakai, T. *Biochemistry* **1985**, *24*, 3199.
(21) DeReimer, L. H.; Meares, C. F.; Goodwin, D. A.; Diamanti, C. I. *J. Med. Chem.* **1979**, *22*, 1619.
(22) Dabrowiak, J. C. *Adv. Inorg. Chem.* **1982**, *4*, 70.
(23) Iitaka, Y.; Nakamura, H.; Nakatoni, T.; Murauka, Y.; Fujii, A.; Takita, T.; Umezawa, H. *J. Antibiot.* **1978**, *31*, 1070.
(24) Sugiura, Y.; Suzuki, T.; Otsuka, M.; Kobayashi, S.; Ohno, M.; Takita, T.; Umezawa, H. *J. Biol. Chem.* **19838** *258*, 1328.
(25) Ishizu, K.; Murata, S.; Miyoshi, K.; Sugiura, Y.; Takita, T.; Umezawa, H. *J. Antibiot.* **1981**, *34*, 996.
(26) Albertini, J. P.; Garnier-Suillerot, A. *Biochemistry* **1982**, *21*, 6777.
(27) Sugiura, Y. *J. Am. Chem. Soc.* **1980**, *102*, 5216.
(28) Sugiura, Y. *J. Am. Chem. Soc.* **1980**, *102*, 5208.
(29) Anthroline, W. E.; Hyde, J. S.; Sealy, R. C.; Petering, D. H. *J. Biol. Chem.* **1984**, *259*, 4437.
(30) Dabrowiak, J. C.; Tsukayama, M. *J. Am. Chem. Soc.* **1981**, *103*, 7543.
(31) Vos, C. M.; Westera, G.; Shipper, D. *J. Inorg. Biochem.* **1980**, *13*, 165.
(32) Oppenheimer, N. J.; Rodriguez, L. O.; Hecht, S. M. *Proc. Natl. Acad. Sci. U.S.A.* **1979**, *76*, 5616.
(33) Oppenheimer, N. J.; Chang, C.; Chang, L. H.; Ehrenfeld, G.; Rodriguez, L. O.; Hecht, S. M. *J. Biol. Chem.* **1982**, *257*, 1606.
(34) Sugiura, Y.; Suzuki, T.; Muraoka, Y.; Umezawa, Y.; Takita, T.; Umezawa, H. *J. Antibiot.* **1981**, *34*, 1232.
(35) Umezawa, H.; Takita, T.; Sugiura, Y.; Otsuka, M.; Kobayashi, S.; Ohno, M. *Tetrahedron* **1984**, *40*, 501.
(36) Sugiyama, H.; Kilkuskie, R. E.; Chang, L. H.; Ma, L. T.; Hecht, S. M.; van der Marcel, G.; van Boom, J. H. *J. Am. Chem. Soc.* **1986**, *108*, 3852.
(37) Sugiyama, H.; Kilkuskie, R. E.; Hecht, S. M.; van der Marcel, G.; van Boom, J. H. *J. Am. Chem. Soc.* **1985**, *107*, 5983.
(38) Takita, T.; Umezawa, Y.; Saito, S.; Morishima, H.; Umezawa, H.; Muraoka, Y.; Suzuki, M.; Otsuka, M.; Kobayashi, S.; Ohno, M. *Tetrahedron Lett.* **1981**, *22*, 671.
(39) Aoyagi, Y.; Suguna, H.; Murugeson, N.; Ehrenfeld, G. M.; Chang, L. H.; Ohgi, T.; Shekhoni, M. S.; Kirup, M. P.; Hecht, S. M. *J. Am. Chem. Soc.* **1982**, *104*, 5237.
(40) Chien, M.; Grollman, A. P.; Horwitz, S. B. *Biochemistry* **1977**, *16*, 3641.
(41) Povirk, L. F.; Hogan, M.; Dattagupta, N. *Biochemistry* **1979**, *18*, 96.
(42) Waring, M. J. *Ann. Rev. Biochem.* **1981**, *50*, 159.
(43) Booth, T. E.; Sakai, T. T.; Glickson, J. D. *J. Biol. Chem.* **1983**, *258*, 4211.
(44) Sakai, T. T.; Riordan, J. M.; Glickson, J. D.l *Biochemistry* **1982**, *21*, 805.
(45) Sugiura, Y.; Suzuki, T. *J. Biol. Chem.* **1982**, *257*, 10544.
(46) Mascharak, P. K.; Sugiura, Y.; Kuwahara, J.; Suzuki, T.; Lippard, S. J. *Proc. Natl. Acad. Sci. U.S.A.* **1983**, *80*, 6795.
(47) Huang, C. H.; Galvan, L.; Crooke, S. T. *Biochemistry* **1980**, *19*, 1761.
(48) Kross, J.; Henner, W. D.; Hecht, S. M.; Haseltine, W. A. *Biochemistry* **1982**, *21*, 4310.
(49) Mirabelli, C. K.; Ting, A.; Huang, C. H.; Mong, S.; Crooke, S. T. *Cancer Res.* **1982**, *42*, 2779.
(50) Dickerson, R. E. In *Mechanism of DNA Damage and Repair: Implications for Carcinogenesis and Risk Assessment in Basic Life Sciences*; Smi, M. G., Grossman, L., Eds.; Plenum: New York, 1986; Vol. 38, p 245.
(51) Kowabara, M.; Youn, C.; Ooyne, T.; Thederath, T.; Sigman, D. S. *Biochemistry* **1986**, *25*, 7401.
(52) Dasgupta, D.; Goldberg, I. H. *Biochemistry* **1985**, *24*, 6913.
(53) Sausville, E. A.; Stein, R. W.; Peisach, J.; Horwitz, S. B. *Biochemistry* **1978**, *17*, 2746.
(54) Sausville, E. A.; Peisach, J.; Horwitz, S. B. *Biochem. Biophys. Res. Commun.* **1976**, *73*, 814.
(55) Ishida, R.; Takahashi, T. *Biochem. Biophys. Res. Commun.* **1975**, *66*, 1432.
(56) Onishi, T.; Iwata, H.; Takagi, Y. *J. Biochem. (Tokyo)* **1975**, *77*, 745.
(57) Haidle, C. W.; Weiss, K. K.; Kuo, M. T. *Mol. Pharmacol.* **1972**, *8*, 531.
(58) Kuo, M. T.; Haidle, C. W. *Biochim. Biophys. Acta* **1974**, *335*, 109.
(59) McMurray, T. J.; Groves, J. T. In *Cyt-P_{450}: Structure, Mechanism and Biochemistry*; Ortiz de Montellano, P., Ed.;

Plenum: New York, 1985; Chapter 1, pp 1–28.
(60) Hager, L. P.; Doubek, D. L.; Silverstein, R. M.; Lee, T. T.; Thomas, J. A.; Hargis, J. H.; Martin, J. C. In *Oxidase and Related Redox Systems*; King, T. E., Mason, H. S., Morrison, M., Eds.; University Park: Baltimore, 1973; Vol. 1, pp 311–332.
(61) Collman, J. P.; Kodadek, T.; Raybuck, S. A.; Brauman, J. I.; Papazian, L. M. *J. Am. Chem. Soc.* **1985**, *107*, 4343.
(62) Groves, J. T.; Nemo, T. E.; Myers, R. S. *J. Am. Chem. Soc.* **1979**, *101*, 1032.
(63) Groves, J. T.; Haushalter, R. C.; Nakamura, M.; Nemo, T. E.; Evans, B. J. *J. Am. Chem. Soc.* **1981**, *103*, 2884.
(64) Burger, R. M.; Peisach, J.; Horwitz, S. B. *J. Biol. Chem.* **1981**, *256*, 11636.
(65) Burger, R. M.; Kent, T. A.; Horwitz, S. B.; Munck, E.; Peisach, J. *J. Biol. Chem.* **1983**, *258*, 1559.
(66) Sugiura, Y.; Kikuchi, T. *J. Antibiot.* **1979**, *31*, 1310.
(67) Kuramochi, H.; Takahashi, K.; Takita, T.; Umezawa, H. *J. Antibiot.* **1981**, *34*, 576.
(68) Burger, R. M.; Horwitz, S. B.; Peisach, J.; Wittenberg, J. B. *J. Biol. Chem.* **1979**, *254*, 12299.
(69) Rabow, L. E.; Stubbe, J.; Kozarich, J. W.; Gerlt, J. A. *J. Am. Chem. Soc.* **1986**, *108*, 7130.
(70) McCandlish, E.; Miksztal, B. R.; Nuppa, M.; Quinn, A. E.; Valentine, J. S.; Strong, J. S.; Spiro, T. G. *J. Am. Chem. Soc.* **1980**, *102*, 4268.
(71) Burger, R. M.; Blanchard, J. S.; Horwitz, S. B.; Peisach, J. *J. Biol. Chem.* **1985**, *260*, 15406.
(72) Fersht, A. *Enzyme Structure and Mechanism*, 2nd ed.; W. H. Freeman: New York, 1985; p 201.
(73) Guengerich, P. F. *Biochem. Biophys. Res. Commun.* **1986**, *138*, 193.
(74) Takita, T.; Muraoka, Y.; Nakatoni, T.; Fujii, a.; Itaka, Y.; Umezawa, H. *J. Antibiot.* **1978**, *31*, 1073.
(75) Dabrowiak, J. C.; Greenaway, F. T.; Santillo, F. S.; Crooke, S. T. *Biochem. Biophys. Res. Commun.* **1979**, *91*, 721.
(76) Padbury, G.; Sligar, S. A. *J. Biol. Chem.* **1985**, *260*, 7820.
(77) Poulos, T. *Pept. Prot. Rev.* **1985**, *4*, 115–171. Poulos, T. L.; Kraut, J. *J. Biol. Chem.* **1980**, *255*, 8199
(78) Poulos, T.; Finzel, B. C.; Gunsalus, I. C.; Wagner, G. C.; Kraut, J. *J. Biol. Chem.* **1985**, *260*, 16122.
(79) White, R. E.; Coon, M. J. *Ann. Rev. Biochem.* **1980**, *49*, 315.
(80) Guengerich, F. P.; MacDonald, T. L. *Acc. Chem. Res.* **1984**, *17*, 9.
(81) Katopodis, A. C.; Wimalasena, K.; Lee, J.; May, S. M. *J. Am. Chem. Soc.* **1984**, *106*, 7928.
(82) Heimbrook, D. C.; Mulholland, R. L.; Hecht, S. M. *J. Am. Chem. Soc.* **1986**, *108*, 7839.
(83) Murugeson, N.; Hecht, S. M. *J. Am. Chem. Soc.* **1985**, *107*, 493.
(84) Murugeson, N.; Ehrenfeld, G. M.; Hecht, S. M. *J. Biol. Chem.* **1982**, *257*, 8600.
(85) Ehrenfeld, G. M.; Murugeson, N.; Hecht, S. M. *Inorg. Chem.* **1984**, *23*, 1496.
(86) Lee, W. A.; Bruice, T. A. *J. Am. Chem. Soc.* **1985**, *107*, 513.
(87) Traylor, T. G.; Lee, W. A.; Stynes, D. V. *J. Am. Chem. Soc.* **1984**, *106*, 755.
(88) Ortiz de Montellano, P. R., Ed. *Cytochrome P_{450}: Structure, Mechanism and Biochemistry*; Pletnum: New York, 1985.
(89) Burger, R. M.; Peisach, J.; Blumberg, W. E.; Horwitz, S. B. *J. Biol. Chem.* **1979**, *254*, 10906.
(90) Lown, J. W.; Joashua, A. V. *Biochem. Pharmacol.* **1980**, *29*, 251.
(91) Oberley, L. W.; Buether, G. R. *FEBS Lett.* **1979**, *97*, 47.
(92) Conor, H. D.; Fisher, V.; Mason, R. P. *Biochem. Biophys. Res. Commun.* **1986**, *141*, 614.
(93) Kittaka, A.; Sugano, Y.; Otsuka, M.; Ohno, M.; Sugiura, Y.; Umezawa, H. *Tetrahedron Lett.* **1986**, *27*, 3631.
(94) Sugano, Y.; Kittaka, A.; Otsuka, M.; Ohno, M.; Sugiura, Y.; Umezawa, H. *Tetrahedron Lett.* **1986**, *27*, 3635.
(95) Otsuka, M.; Kittaka, A.; Ohno, M.; Suzuki, T.; Kuwahara, J.; Sugiura, Y.; Umezawa, H. *Tetrahedron Lett.* **1986**, *27*, 3639.
(96) Rodriguez, L. O.; Hecht, S. M. *Biochem. Biophys. Res. Commun.* **1982**, *104*, 1470.
(97) Galvin, L.; Huang, C. H.; Prestayko, A. W.; Stout, J. T.; Evans, J. E.; Crooke, S. T. *Cancer Res.* **1981**, *41*, 5103.
(98) Uesugi, S.; Shida, T.; Ikehara, M.; Kobayashi, Y.; Kyogoku, Y. *Nucleic Acids Res.* **1984**, *12*, 1581.
(99) Murugeson, N.; Xu, C.; Ehrenfeld, G. M.; Sugiyama, H.; Kilkuskie, R. E.; Rodriguez, L. O.; Chang, L. H.; Hecht, S. M. *Biochemistry* **1985**, *24*, 5735.
(100) Burger, R. M.; Peisach, J.; Horwitz, S. B. *J. Biol. Chem.* **1982**, *257*, 8612.
(101) Wu, J.; Kozarich, J. W.; Stubbe, J. *J. Biol. Chem.* **1983**, *258*, 4694.
(102) Wu, J. C.; Kozarich, J. W.; Stubbe, J. *Biochemistry* **1985**, *24*, 7562.
(103) Ingold, K. U. *Acc. Chem. Res.* **1969**, *2*, 1.
(104) Grollman, A. P.; Takeshita, M.; Pillai, K. M.; Johnson, F. *Cancer Res.* **1985**, *45*, 1127.
(105) Ajmera, S.; Wu, J. C.; Worth, L.; Rabow, L. E.; Stubbe, J.; Kozarich, J. W. *Biochemistry* **1986**, *25*, 6586.
(106) Bothe, E.; Behrens, G.; Böhm, E.; Sethuram, B.; Schulte-Frohlinde, D. *Int. J. Radiat. Biol. Relat. Stud. Phys. Chem. Med.* **1986**, *49*, 57.
(107) Schulte-Frohlinde, D.; Behrens, G.; Önal, A. *Int. J. Radiat. Biol. Relat. Stud. Phys. Chem. Med.* **1986**, *50*, 103.
(108) von Sonntag, C. *Int. J. Radiat. Biol. Relat. Stud. Phys. Chem. Med.* **1984**, *46*, 507.
(109) Howard, J. A.; Ingold, K. O. *Can. J. Chem.* **1962**, *40*, 185.
(110) Anderson, G. H.; Smith, J. G. *Can. J. Chem.* **1968**, *46*, 1553.
(111) Bassey, M.; Bunton, C. A.; Davis, A. G.; Lewis, T. A. *J. Chem. Soc.* **1955**, 2471.
(112) Burtzlatt, G.; Felher, V.; Hubner, H.; Pritzkaw, W.; Rale, W. *J. Prakt. Chem.* **1965**, *28*, 305.
(113) Khorash, M. S.; Fond, A.; Nudenberg, W. *J. Org. Chem.* **1950**, *15*, 748.
(114) Mayer, R.; Que, L. *J. Biol. Chem.* **1984**, *259*, 10356.
(115) Walsh, T. A.; Ballou, D. P.; Mayer, R.; Que, L., Jr. *J. Biol. Chem.* **1983**, *258*, 14422.
(116) Saito, I.; Morii, T.; Matsuura, T. *Nucleic Acids Symp. Ser.* **1983**, *n12*, 95.
(117) Schrieber, S. L.; Liew, W. *Tetrahedron Lett.* **1983**, *24*, 2363. Criegee, R. *Ber. Dtsch. Chem. Ges. A* **1944**, *77*, 772.
(118) McGall, G.; Rabow, L. E.; Stubbe, J.; Kozarich, J. W. *J. Am. Chem. Soc.* **1987**, *109*, 283.
(119) Rendina, A. R.; Hermes, J. D.; Cleland, W. W. *Biochemistry* **1984**, *23*, 5148.
(120) Burger, R. M.; Projan, S. J.; Horwitz, S. B.; Peisach, J. *J. Biol. Chem.* **1986**, *261*, 15955.
(121) Ashley, G. W.; Stubbe, *J. Pharm. Ther.* **1986**, *301*.
(122) Groves, J. T.; McClusky, G. A. In *Oxygen: Clinical and Biochemical Aspects*; Caughey, W. S., Ed.; Academic: New York, 1982.
(123) Rabow, L.; Stubbe, J.; Kozarich, J. W.; Gerlt, J. A. *J. Am. Chem. Soc.* **1986**, *108*, 7130.
(124) Sugiyama, H.; Xu, C.; Murugesan, N.; Hecht, S. Am. *J. Am. Chem. Soc.* **1985**, *107*, 4104.
(125) Rao, U. Y.; Ice, R. D.; Jones, J. D.; Beirwaites, W. H. *J. Nucl. Med.* **1975**, *16*, 127.
(126) Nunn, A. D. *Eur. J. Nucl. Med.* **1977**, *2*, 53.
(127) Chang, C. H.; Dallas, J. L.; Meares, C. F. *Biochem. Biophys. Res. Commun.* **1983**, *110*, 959.
(128) Chang, C. H.; Meares, C. F. *Biochemistry* **1982**, *21*, 6332.
(129) Vos, C. M.; Westera, G.; von Zanten, B. *J. Inorg. Biochem.* **1980**, *12*, 45.
(130) Vos, C. M.; Westera, G. *J. Inorg. Biochem.* **1981**, *15*, 253.
(131) Rasker, J. J.; Beekhuis, H.; van de Poll, M. A. P. C.; Versluis, A.; Jergens, H.; Woldring, M. G. *Nucl. Med.* **1978**, *17*, 238.
(132) Chang, K. H.; Meares, C. F. *Biochemistry* **1984**, *23*, 2268.
(133) Wensel, T. G.; Chang, C. H.; Meares, C. F. *Biochemistry* **1985**, *24*, 3060.
(134) Adamson, A. W. *Coord. Chem. Rev.* **1968**, *3*, 169.
(135) Adamson, A. W. *Pure Appl. Chem.* **1979**, *51*, 313.
(136) Janicek, M. F.; Haseltine, W. A.; Henner, W. D. *Nucleic Acids Res.* **1985**, *13*, 9011.
(137) Giloni, L.; Takeshita, M.; Johnson, F.; Grollman, A. *J. Biol. Chem.* **1981**, *256*, 8608.
(138) von Sonntag, C.; Hagen, V.; Schön-Bopp, A.; Schulte-Frohlinde, D. In *Advances in Radition Biology*; Lett, J. T., Adler, H., Eds.; Academic: New York, 1981: Vol. 9, pp 109–142.
(139) Deeble, D. J.; von Sonntag, C. *Int. J. Radiat. Biol. Relat. Stud. Phys. Chem. Med.* **1986**, *49*, 927.
(140) Ehrenfeld, G. M.; Murugeson, N.; Hecht, S. M. *Inorg. Chem.* **1984**, *23*, 1496.
(141) Burger, R. M.; Freedman, J. H.; Horwitz, S. B.; Peisach, J. *Inorg. Chem.* **1984**, *23*, 2215.
(142) Suzuki, T.; Kuwahara, J.; Goto, M.; Sugiura, Y. *Biochim. Biophys. Acta* **1984**, *824*, 330.
(143) Ehrenfeld, G. M.; Rodriguez, L. O.; Hecht, S. M.; Chang, C.; Basus, V. J.; Oppenheimer, J. J. *Biochemistry* **1985**, *24*, 81.
(144) Suzuki, T.; Kuwahara, J.; Sugiura, Y. *Biochemistry* **1985**, *24*, 4719.
(145) Antholine, W. E.; Salaimon, D.; Saryon, L. A.; Petering, D. H. *J. Inorganic Biochem.* **1982**, *17*, 75.
(146) Ishizuka, M.; Takayama, H.; Takeuchi, T.; Umezawa, H. *J. Antibiot. Ser. A* **1967**, *20*, 15.
(147) Umezawa, H.; Ishizuka, M.; Kimura, K.; Iwonda, J.; Takeuchi, T. *J. Antibiot.* **1968**, *21*, 592.
(148) Takahashi, K.; Yoshioka, O.; Matsuda, A.; Umezawa, H. *J. Antibiot.* **1977**, *30*, 861.
(149) Freedman, J. H.; Horwitz, S. B.; Peisach, J. *Biochemistry* **1982**, *21*, 2203.
(150) Kilkuskie, R. E.; MacDonald, T. L.; Hecht, S. M. *Biochemistry* **1984**, *23*, 6165.
(151) Schuelen, M. E.; Kappus, H.; Thyssen, D.; Schmidt, C. G. *Biochem. Pharmacol.* **1981**, *30*, 3385.
(152) Suzuki, H.; Nagai, K.; Kutsu, E. A.; Yamaki, H.; Tanaka, N.; Umezawa, H. *J. Antibiot.* **1970**, *23*, 473.

(153) Sausville, E. A.; Peisach, J.; Horwitz, S. B. *Biochemistry* **1978**, *17*, 2740.
(154) Reich, K. A.; Marshall, L. E.; Graham, D. R.; Sigman, D. S. *J. Am. Chem. Soc.* **1981**, *103*, 3852.
(155) Kuwabara, M.; Youn, C.; Ooyne, T.; Thederah, T.; Sigman, D. S. *Biochemistry* **1986**, *25*, 7401.
(156) Pope, L. E.; Sigman, D. S. *Proc. Natl. Acad. Sci. U.S.A.* **1984**, *81*, 3.
(157) Graham, D. R.; Marshall, L. E.; Reich, K. A.; Sigman, D. S. *J. Am. Chem. Soc.* **1980**, *102*, 5421.
(158) Kopka, M. L.; Youn, C.; Goodsell, D.; Pjura, D.; Dickerson, R. E. *J. Mol. Biol.* **1985**, *183*, 553.
(159) McClarin, J. A.; Frederick, C. A.; Wong, B. C.; Greere, P.; Boyer, H. W.; Grable, J.; Rosenberg, J. M. *Science (Washington, D.C.)* **1986**, *234*, 1526.
(160) Walling, C. *Acc. Chem. Res.* **1975**, *8*, 125.
(161) Hertzberg, R. P.; Dervan, P. B. *Biochemistry* **1984**, *23*, 3934.
(162) Henner, W. D.; Rodriguez, L. O.; Hecht, S. M.; Haseltine, W. A. *J. Biol. Chem.* **1983**, *258*, 711.
(163) Uesugi, S.; Shida, T.; Ikehara, M.; Kobayashi, Y.; Kyogoku, Y. *J. Am. Chem. Soc.* **1982**, *104*, 5494.
(164) Hertzberg, R. P.; Dervan, P. B. *J. Am. Chem. Soc.* **1982**, *104*, 313.
(165) Van Dyke, M. M.; Dervan, P. B. *Science (Washington, D.C.)* **1984**, *225*, 1122.
(166) Rush, J. D.; Koppenol, W. H. *J. Biol. Chem.* **1986**, *261*, 6730.
(167) Balasubramanian, P. N.; Bruice, T. C. *J. Am. Chem. Soc.* **1986**, *108*, 5495.
(168) Shiga, T. *J. Phys. Chem.* **1965**, *69*, 3805.
(169) Cahill, A. E.; Taube, H. *J. Am. Chem. Soc.* **1952**, *74*, 2312.
(170) Walling, C.; Portoh, R. E.; Weil, T. *Proc. Natl. Acad. Sci. U.S.A.* **1975**, *72*, 140.
(171) Walling, C.; Kurz, M.; Schugar, H. J. *Inorg. Chem.* **1970**, *9*, 931.
(172) Duplaa, A. M.; Téoule, R. *Int. J. Radiat. Biol. Relat. Stud. Phys. Chem. Med.* **1985**, *48*, 19.
(173) Schulte-Frohlinde, D.; Bothe, E. *Z. Naturforsch. C: Biosci.* **1984**, *39C*, 315.
(174) Schulte-Frohlinde, D.; Behrens, G.; Onal, A. *Int. J. Radiat. Biol. Relat. Stud. Phys. Chem. Med.* **1986**, *50*, 103.
(175) Henner, W. D.; Grunberg, S. M.; Haseltine, W. A. *J. Biol. Chem.* **1982**, *257*, 11750.
(176) LeMaire, D. G. E.; Bothe, E.; Schulte-Frohlinde, D. *Int. J. Radiat. Biol. Relat. Stud. Phys. Chem. Med.* **1984**, *45*, 351.
(177) Beesk, F.; Dizduroglu, M.; Schulte-Frohlinde, D.; von Sonntag, C. *Int. J. Radiat. Biol. Relat. Stud. Phys. Chem. Med.* **1979**, *36*, 565.
(178) Behrens, G.; Koltzenburg, G.; Schulte-Frohlinde, D. *Z. Naturforsch. C.: Biosci.* **1982**, *37C*, 1205.
(179) Behrens, G.; Koltzenburg, G.; Ritter, A.; Schulte-Frohlinde, D. *Int. J. Radiat. Biol. Relat. Stud. Phys. Chem. Med.* **1978**, *33*, 163.
(180) Akhlaq, M.; Schuchmann, H.; von Sonntag, C. *Int. J. Radiat. Biol. Relat. Stud. Phys. Chem. Med.* **1987**, *51*, 91.
(181) Boon, P. J.; Cullis, P. M.; Symons, M. C. R.; Wren, B. W. *J. Chem. Soc., Perkin Trans. 2* **1984**, 1343.
(182) Antholine, W. E.; Petering, D. H. *Biochem. Biophys. Res. Commun.* **1979**, *90*, 384.
(183) Burger, R. M.; Peisach, J.; Blumberg, W. E.; Horwitz, S. B. *J. Biol. Chem.* **1979**, *254*, 10906.
(184) Ebel, R. E.; O'Keefe, D. H.; Peterson, J. A. *FEBS Lett.* **1975**, *55*, 198.
(185) Chevion, M.; Stern, A.; Peisach, J.; Simon, S. *Biochemistry* **1978**, *17*, 1745.
(186) McCarthy, M. B.; White, R. G. *J. Biol. Chem.* **1983**, *258*, 9153.
(187) Miwa, G. T.; Walsh, J. S.; Kedderis, G. L.; Hollenberg, P. T. *J. Biol. Chem.* **1983**, *258*, 14445.
(188) Heimbrook, P. C.; Murray, R. I.; Egeberg, K. D.; Sligar, S. G. *J. Am. Chem. Soc.* **1984**, *106*, 1514.
(189) Hager, L. P.; Morris, D. R.; Brown, F. S.; Eberwer, H. *J. Biol. Chem.* **1966**, *251*, 1769.
(190) Kedderis, G. L.; Koop, D. R.; Hollenberg, P. F. *J. Biol. Chem.* **1980**, *255*, 10174.
(191) Isildar, M.; Schuchmann, D.; Schulte-Forhlinde, D.; von Sonntag, C. *Int. J. Radiat. Biol. Relat. Stud. Phys. Chem. Med.* **1981**, *40*, 347.
(192) Dizduroglu, M.; Schulte-Frohlinde, D.; von Sonntag, C. *Z. Naturforsch. C: Biosci.* **1977**, *32C*, 1021.
(193) Saito, I.; Morii, T.; Matsuura, T. *J. Org. Chem.* **1987**, *52*, 1008.
(194) Melnyk, D. L.; Horwitz, S. B.; Peisach, J. *Biochemistry* **1981**, *20*, 5327.
(195) Goyne, T.; Sigman, D. S. *J. Am. Chem. Soc.* **1987**, *109*, 2846.
(196) Ehrenfeld, G. M.; Shipley, J. B.; Heimbrook, D. C.; Sugiyama, H.; Long, E. C.; van Boom, J. H.; van der Marel, G. A.; Oppenheimer, N. J.; Hecht, S. M. *Biochemistry* **1987**, *26*, 931–942.